2024-06

Design and Optimization of Non-Invasive Brain Stimulation Systems: Case for Depression Recovery

Sintayehu, Kelemu Fekede

BAHIR DAR UNIVERSITY

BAHIR DAR INSTITUTE OF TECHNOLOGY

SCHOOL OF RESEARCH AND GRADUATE STUDIES

FACULTY OF ELECTRICAL AND COMPUTER ENGINEERING

Biomedical Engineering Program

MSc thesis on:

Design and Optimization of Non-Invasive Brain Stimulation Systems: Case for Depression Recovery

By

Sintayehu Kelemu Fekede

June 2024

Bahir Dar, Ethiopia

BAHIR DAR UNIVERSITY

BAHIR DAR INSTITUTE OF TECHNOLOGY

SCHOOL OF RESEARCH AND GRADUATE STUDIES

FACULTY OF ELECTRICAL AND COMPUTER ENGINEERING

Biomedical Engineering Program

MSc thesis on:

Design and Optimization of Non-Invasive Brain Stimulation Systems: Case for Depression Recovery

By

Sintayehu Kelemu Fekede

A thesis submitted

in Partial Fulfillment of the Requirements for the Degree of Master of Science in Biomedical Engineering

Main Advisor: Dr. Amare Kassaw Yimer (PhD)

June 2024

Bahir Dar, Ethiopia

Declaration

This is a declaration that the thesis," **Design and Optimization of Non-Invasive Brain Stimulation Systems: Case for Depression Recovery"** submitted as partial fulfillment of the requirements for the Degree of Master of Science in "Biomedical Engineering" at the Faculty of Electrical and Computer Engineering, Bahir Dar Institute of Technology, Bahir Dar university is a record of my original work and has never been submitted to this or any other institution to obtain any other degree or certification. The resource and support I received throughout this investigation have been properly acknowledged.

Sintayehu Kelemu Fekede	----  ----	19/07/2024
Name of candidate	**Signature**	**Date**

Approval of Thesis for defense

I hereby confirm that the changes required by the examiners have been carried out and incorporated in the final thesis.

Name of Student: Sintayehu Kelemu Fekede, Signature: ______ Date: 19/07/2024

As members of the board of examiners, we examined this thesis entitled "**Design and Optimization of Non-Invasive Brain Stimulation Systems: Case for Depression Recovery**" by Sintayehu Kelemu. We hereby certify that the thesis is accepted for fulfilling the requirements for the award of the degree of Master of Science in Biomedical Engineering.

Board of Examiners

Dr. Amare Kassaw		19/07/2024
Name of Advisor	**Signature**	**Date**
Dr. Eng. Getachew Alemu Wondim		19 / 07 / 2024
Name of External Examiner	**Signature**	**Date**
Dr. Selamawit Workalemahu		19/07/2024
Name of Internal Examiner	**Signature**	**Date**
Fanuel Melak		30/07/2024
Name of Chairperson	**Signature**	**Date**
Lijalem Getnet Ayalew		30/07/2024
Name of Chair Holder	**Signature**	**Date**
Tekelay Mulu Beza (PhD)		30/07/2024
Name of Faculty Dean	**Signature**	**Date**

Mezigebu Getinet Yenealem
Assistant Proffessor (Ph.D)
Post Graduate Coordinator

Acknowledgments

I am grateful to the Almighty God for His mercies, resources, sustenance, and most significantly, His love and faithfulness during my educational path to this MSc level. His kindness has helped me prosper and thrive in all of my academic endeavors.

My heartfelt thanks go to my kind, supportive, and modest supervisor, Dr. Amare Kassaw Yimer (PhD), for all of his invaluable advice and contributions throughout my thesis. Doctor, I sincerely appreciate your encouragement, respect your counsel, and kind remarks, which more than illustrate my path through this thesis and a high degree of independence. Furthermore, I'd like to thank BIT for the opportunity and the entire BIT community for their support and assistance. Finally, I want to thank my beloved families and friends for always being there for me.

Abstract

According to the World Health Organization, by 2022, nervous system disorders is the second leading cause of death worldwide and the leading cause of disability-adjusted life years. The two primary diagnostic subgroups of common mental diseases are depressive disorder/depression and anxiety disorder. Depression is the leading cause of disability worldwide (7.5% of all years with disability), and anxiety disorders are ranked sixth (3.4%). Furthermore, depression is a major factor in the approximately 800,000 suicide fatalities that occur each year. According to World Health Organization data, by 2022, approximately 322 million people worldwide with depression, and from those 4,480,113 total cases are found in Ethiopia. Brain disorders are thought to arise from abnormal neural activities, and neuromodulation methods are becoming increasingly popular because they can directly manipulate these neural circuits. Non-invasive brain stimulation via transcranial magnetic stimulation, which uses a magnetic pulse to activate a specific brain region, or transcranial direct current stimulation , which uses a mild electrical current to modulate neuronal activity, is effective for research and have potential therapeutic applications in health facilities. For the exploration of neurophysiology, cognitive, emotional, and other behavioral domains in healthy controls, as well as for the treatment of patients suffering from various neuropsychiatric illnesses, Transcranial magnetic stimulation and direct current stimulation are regarded as safe and well-tolerated therapies. Transcranial magnetic stimulation activates deep brain regions responsible for depression, resulting in significant improvement for patients, including those who had tried multiple antidepressant cycles and it is a novel, non-invasive, and effective depression treatment.

In this thesis, we design, simulate and analyze non-invasive brain stimulation system for depression recovery. We first assess and investigate the current impact level of depressive disorder in the local community, as well as the challenges and obstacles to treatment, and then we review the effectiveness of non-invasive brain stimulation for depression treatments. Then we use fast electrical and electromagnetic field distribution computational model software packages to design and simulate non-invasive transcranial magnetic brain stimulation for the treatment of brain depression, as well as to optimize and analyze the design and simulation outputs.

Keywords: *Brain depression, Computational model, NIBS, Mental disorder, TDCS, TMS*

Contents

List of Figures

List of Tables

Abbreviations and symbols

Abbreviations

ADM	Auxiliary Dipole Method
ACC	Anterior Cingulate Cortex
BEM	Boundary Element Method
BEM-FMM	Fast Multipole Boundary Element Method
BIE	Boundary Integral Equation
CSF	Cerebrospinal Fluid
DLPFC	Dorsolateral Prefrontal Cortex
EEG	Electroencephalograph
EFM	Element Free Method
FEM	Finite Element Method
FDM	Finite Difference Method
FMM	Fast Multipole Method
GM	Gray Matter
MDD	Major Depression Disorder
MRI	Magnetic Resonance Imaging
fMRI	Functional Magnetic Resonance Imaging
NIBS	Non-Invasive Brain Stimulation
ODE	Ordinary Differential Equation
PDE	Partial Differential Equations
PIE	Partial Integral Equations

ROI	Region of Interest
RTMS	Repetitive Transcranial Magnetic Stimulation
SimNIBS	Simulation of Non-Invasive Brain stimulator
TBS	Transcranial Brain Stimulation
TDCS	Transcranial Direct Current Stimulation
TES	Transcranial Electrical Stimulation
TMS	Transcranial Magnetic Stimulation
WM	White Matter
WHO	World Health Organization

List of Symbols

ω	Angular frequncy
$\rho(\boldsymbol{r})$	Charge density
σ	Conductivity of the human brain layers
J	Current density vector
D	Displacement vector
E	Electric field strength
f	Frequncy
B	Magnetic field strength
A	Magnetic vector potential
εr	Relative permittivity
εo	Vacuum permitivity
∇	Vector operator
S/m	Siemens per meter
V/m	Voltage per meter

CHAPTER ONE

Introduction

1.1 Background

Neurological disorders are the main cause of disability-adjusted life year and the biggest cause of death worldwide, accounting for 9 million fatalities per year [1], [2].

According to the WHO prevalence of mental disorder report in 2019, [1] one out of every eight individuals, or 970 million people worldwide, suffered from a mental disorder, the most frequent of which were anxiety and depression. The COVID-19 outbreak resulted in a significant increase in the number of persons suffering from anxiety and depression in 2020. Major depressive disorder(MDD) significantly affects the person quality of life [3].

In addition, the WHO estimates that 280 million individuals worldwide suffer from depression, accounting for around 5% of the global adult population [1]. Major depression accounts for 4.3% of total disability-adjusted life years, ranking third among all disorders. According to the WHO's 2030 forecasts, serious depression will account for 6.2% of the total DALY burden, and patients with MDD have twice the death rate as the general population.

Depression is ranked by WHO as the single largest contributor to global disability (7.5% of all years lived with disability); anxiety disorders are ranked 6 th (3.4%) and it is also a major contributor to suicide deaths, which number close to 800 000 per year [2]. According to the WHO African region country estimate for 2022, the prevalence of depression and anxiety disorders in Ethiopia is 4,480,113 and 3,139,003, respectively [1], [2].

Globally, 52.9 million children younger than 5 years had developmental disabilities and 95% of these children lived in low- and middle-income countries [3]. Neuropsychiatric disorders are a leading source of disability and require novel treatments that target the mechanisms of disease [3], [4].

Neuromodulation methods are indispensable for investigating brain function and treating several neurological and psychiatric conditions [4]. These methods intervene directly with neural activity through a wide array of mechanisms, such as electromagnetic fields. Noninvasive brain stimulation(NIBS) is a valuable tool for interventional neurophysiology applications, modulating brain activity in a specific, distributed cortico-subcortical network to induce controlled and controllable behavioral manipulations; and for focal

neuropharmacology delivery, via neurotransmitter release in specific neural networks and the induction of focal gene expression, which may result in a specific behavioral impact [2]. Given the numerous ongoing clinical trials being conducted in a wide range of disorders, NIBS is a feasible treatment for several medical ailments. The therapeutic utility of noninvasive brain stimulation has been claimed in the literature for psychiatric disorders, such as depression, acute mania, bipolar disorders, hallucinations, obsessions, schizophrenia, catatonia, posttraumatic stress disorder, or drug craving; neurologic diseases, such as Parkinson's disease, dystonia, tics, stuttering, tinnitus, spasticity, or epilepsy; rehabilitation of aphasia or hand function after stroke; and pain syndromes [2], [3], [4], [5].

1.1.1 Brain Stimulation

A variety of mental illnesses can be treated with brain-stimulating therapies. Brain stimulation therapies involve directly electrically stimulating or inhibiting the brain. NIBS became an innovative tool for neurophysiologic research, psychological and cognitive investigation, and, ultimately, clinical treatment of a wide spectrum of neuropsychiatric conditions. Indeed, the two primary NIBS techniques TMS and TDCS have emerged as the cornerstones of clinical neuroscience as instruments for studying cognitive and behavioral processes. On the other hand, as the acronym NIBS literally indicates, TMS and DCS are considered safe and well-tolerated interventions for the investigation of neurophysiology, cognitive, affective, and other behavioral domains in healthy controls, as well as for the treatment of patients affected by different neuropsychiatric disorders [2], [5]. Many clinicians and patients believe that clinical use of NIBS as therapeutic interventions, TMS and DCS are better tolerated than many psychotropic drugs due to their lack of systemic side-effects, such as weight gain and sexual dysfunctions, which are frequently responsible for poor therapy compliance and treatment withdrawal in medicated patients [6]. TMS allows neurostimulation and neuromodulation, while DCS is a pure neuromodulator application [2]. TMS and DCS allow diagnostic and interventional neurophysiology applications and focal neuropharmacology delivery. TMS is a popular neurostimulation method that employs magnetic induction to generate current in the brain remotely through a coil placed next to the subject's head. It is noninvasive and noncontact [2]**.** TMS activates deep brain regions which are responsible for depression, generating

significant improvement for patients, including those who tried several cycles of antidepressants. TMS is a novel, non-invasive, and highly effective treatment for depression.

1.1.2 Design Principles of Transcranial Brain Stimulation

Transcranial Brain Stimulation (TBS) methods allow for modulating brain activity in a non-invasive fashion and with minimal side effects [6]. TMS, which utilizes a magnetic coil to create an electric field in the brain by electromagnetic induction, and transcranial electric stimulation (TES), which uses electrodes inserted in the scalp to create an electric field in the brain, are the two main types of TBS.

TMS is a neurophysiological technique that allows a noninvasive, painless stimulation of the human brain through the intact scalp [2], [7] and uses a large, time-varying electric current, passing through a coil placed close to the head [6] as shown the figure 1 below.

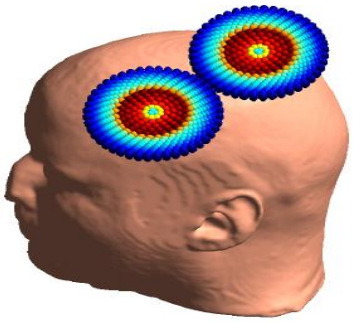

Figure 1: A Computational model of TMS

Depending on where the coil is placed, TMS can target various parts of the brain. Since the output produced by the stimulation of one side's primary motor area can be easily recorded from muscles on the opposite side of the body, TMS effects on motor areas have been better defined than non-motor areas [7].

TMS is based on Faraday's principle of electromagnetic induction, according to which a time-varying magnetic field will induce an electric current [8]. In TMS, a coil composed of copper wire loops encased in plastic receives a short electric current that is passed through a capacitor. A focal magnetic field that is induced perpendicular to the coil plane enters the scalp and the skull without attenuation and produces an electric current [6], [7], [8]. An action potential will be produced if the induced electric current is powerful enough to alter the electrical potential of the conducting surface neuronal membranes [2] ,[8]. That means magnetic stimulators are composed of two main parts: a capacitive high-voltage,

high-current charge-discharge system, and a magnetic stimulating coil system that generates pulsed fields of 1-4 Tesla strength with durations of about a millisecond for single-pulse stimulators and a quarter of a millisecond for rapid stimulators [2].

Because TMS is non-invasive, computational modeling of the electric and magnetic fields within a patient-specific head model is the primary, and sometimes the only method for promoting spatial targeting and/or obtaining a quantitative measure of stimulation intensity.

Thus, in this thesis, we use an alternatively modeling approach for fast, high-resolution simulation of TMS. The mathematical algorithm is based on a direct description of the boundary element method in terms of induced charge density at interfaces, which is naturally paired with the fast multipole method, or BEM-FMM is used to simulate and analyze the computational distribution of electromagnetic fields on the human brain tissue layers. we also simulate and analyze the TMS coil design and also simulate the coil positions on each brain compartments.

1.2 Statement of the Problem

The increasing prevalence of MDD presents a significant public health challenge, affecting millions of individuals worldwide and leading to substantial personal, social, and economic burdens. The current therapy strategy for brain disorders includes antidepressant drugs and psychologists, as well as holy water in low-income and religious countries, which is the most common and first-line treatment for many people. However, because of the scarcity and high cost of antidepressant medicine, more than 75% of people in low- and middle-income countries [14], do not get the full treatment. Furthermore, even if a patient receives antidepressant medication therapy, they will experience common side effects such as low blood pressure, irregular heart rate, nervousness, sexual problems, difficulty sleeping, and seizure, and also the majority of patients will not respond adequately. NIBS is currently a recently proposed method that helps to tolerate alternative treatment for MDD than many antidepressant drugs due to their lack of systemic side effects, effective results with depression, and painless and non-invasive administration. TMS involves the application of magnetic fields to specific brain regions, inducing electric currents that modulate neuronal activity. This method has gained significant attention due to its effectiveness, minimal side effects cost effective, and non-invasiveness. Despite its clinical success, optimizing TMS

for individual patients remains a challenge. This is where computational models play a crucial role. Computational models of TMS involve the use of mathematical and computer simulations to understand and predict the effects of magnetic stimulation on the brain.

As a result, in this thesis, we use the fast computational mathematical algorithm model to design, simulate, and analyze noninvasive brain stimulation/TMS devices that aid in the detection and treatment of the consequences of community MDD.

1.2.1 Main Research Questions

In this regard, the thesis should answer the following research questions

1) What is the impact level of major depressive disorder in the local community?
2) How to model and design and what are the design components of TMS?
3) What are the methods or techniques used to optimize TMS design?
4) What are the methods or techniques applied in TMS simulation and analysis?

1.3 Objectives of the Study

1.3.1 General objective

The main objective of this research is to design, simulate and analyze a computational model of non-invasive transcranial magnetic stimulation systems for the treatment of major depressive disorders.

1.3.2 Specific objectives

- To examine and investigate the impact level of major depressive disorder in the local community, as well as current treatment methods and challenges.
- To describe the computational model and design of a non-invasive transcranial magnetic brain stimulator for depression treatment.
- To identify the level and location of neural activity loss during MDD
- To review literature evidence related to the TMS design principle and treatment method
- To optimize the design results that customized the proposed systems
- To simulate and analyze the results of a non-invasive transcranial magnetic brain stimulation model.

1.4 Significance of the Thesis

According to WHO data for 2021, nervous system illnesses affect over 3 billion people worldwide and account for 9 million deaths each year, making them the second leading cause of death in terms of disability-adjusted life years.

Due to the better tolerated therapeutic interventions than many psychotropic drugs and lack of systemic side-effects, NIBS, is an innovative tool for neurophysiologic research, psychological and cognitive investigation, and, ultimately, clinical treatment of a wide spectrum of neuropsychiatric conditions. From the common non-invasive brain simulator, TMS is more effective stimulator for the treatment of the MDD.

This thesis presents a computational design, simulation, and analysis of, effective therapy, simple-to-use, and an optimized transcranial magnetic brain stimulation that can treat and decrease the prevalence of the MDD in the local community. If the proposed method is implemented, local populations will benefit from reduced antidepressant medication costs, reduced drug side effects, shorter wait times for psychiatric doctors, and faster relief.

Those psychiatry patients that are not responding to antidepression drugs are also treated as well. Since transcranial brain stimulation is non-invasive, there is no chemical insertion into patients' body, the patients are safer from brain damage due to chemical and antidepressant adaptations. On the other hand, psychiatry professionals at healthcare levels are more benefitted from these devices as it helps them to treat patients safely and they can get basic engineering knowledges of brain stimulation with magnetic energy which motivate them for further research. Furthermore, the researcher will improve knowledge of the human brain electrical circuit system, brain loss, and brain stimulation systems and methods of treatments for further research to help the communities.

1.5 The Scope of the Thesis

The first phase of this thesis examined the severity and prevalence of major depressive disorder at the local level in the psychiatric departments of two particular Hospitals, Tibebe Ghion and Felege Hiwot, and also review the present non-invasive transcranial magnetic brain stimulation approaches for depression treatment and their limitations. Then, it describes the system computational design model and simulation of an optimal transcranial magnetic brain stimulator model for depression therapy, and then analyzes the simulator's performances, and ended with concluding.

1.6 Ethical Consideration

The study was carried out after the idea was authorized by the SADK committee at Bahir Dar Institute of Technology, and the Bahir Dar Institute of Technology ethical clearance approval committee granted permission for the research activity. Letters of support were also obtained from the appropriate bodies (Tibebe Gihon Specialized Teaching Hospital and Felege Hiwot Specialized Hospital).

All study participants were told on the trial's goal and advantages, and their consent was obtained orally in advance. Health professionals will guarantee that the study follows ethical norms and legislation governing patient data protection, consent, and confidentiality throughout. Obtain the necessary approvals for the collecting and use of patient data in this study, as well as the proper anonymization and safeguarding of sensitive information.

1.7 Organization of Thesis

The structure of this thesis is defined and organized as follows:

Chapter 1: It includes a problem statement, research questions, ethical clearance and objectives in addition to an introduction and background of the thesis work. It also discusses the significance and rationality of the research.

Chapter 2: Presents a review of the literature on the model design, method of simulation and optimization principles and techniques of TMS system for recovery of MDD.

Chapter 3: Shows the methodology, resources, mathematical computational model, governing equations and tools utilized to support the work, as well as the strategy, technique, and system model.

Chapter 4: It explains collected data analysis, the outcomes and repercussions of putting the plan into action, examines the output of a matlab simulation which includes the distribution of electromagnetic fields, and also illustrate the TMS coil design.

Chapter 5: This section displays the thesis finding and work result conclusion, as well as the thesis limitations and future work.

CHAPTER TWO

Literature Review

Transcranial magnetic stimulation uses a coil placed on the scalp to non-invasively modulate the activity of targeted brain networks via a magnetically induced electric field (E-field), and the E-field induced during TMS is ideally focused on a targeted cortical region of interest [9]. As [9] proposed, to improve TMS computational accuracy and speed, they developed a fast computational auxiliary dipole method as compared to the finite element computational method for determining the best coil position and orientation. The optimal coil placing maximizes the E-field along a predetermined direction or the overall E-field magnitude in the targeted region of interest

According to the author of [10] studies, the Quadruple Butterfly Coil was developed with the main goal of allowing researchers a finer resolution for stimulation, and this new coil aims to decrease the stimulation volume over the cortex rather than achieve deeper brain stimulation. Also, the calculation of the electric field (E-field) and modelling of transcranial magnetic stimulation coils were performed using SEMCAD X, and a quasi-static, low-frequency solver was used for the calculation of the induced electric field in the brain. TMS coil geometry is critical in determining the facility and depth of penetration of the induced electric field that causes stimulation. Clinicians and basic scientists are interested in stimulating a specific area of the brain while preventing surrounding neural networks.

The research work conducted by [3] designs a novel Halo V TMS coil made of conventional Halo and V coils. By examining the distribution of the induced magnetic and electric fields, the impact of the Halo V coil on the human head model in ball form is examined. In order to investigate the distributions of induced electric and magnetic fields, the researchers [3] present a simulation of the Halo V coil mounted on the five-shell spherical human head model using the finite element approach. By contrasting the simulation results with the commercially available Halo-figure eight assembly coil and common single coils like the Halo and V coils, the performance of the proposed Halo V coil is assessed. Simulation results reveal that the Halo V coil has better focality in terms of electric field dispersion compared to other single and assembly stimulation coils.

According to the research conducted by [4] Finite element method (FEM), Boundary element method (BEM), and Finite difference method (FDM) are commonly used for TMS E-field dosimetry and sensitivity analysis to TMS setup settings. Modelling and numerical mistakes restrict the accuracy of these procedures. Numerical error, unlike modelling mistake, can be minimized and not have a substantial impact on accuracy.

Computational modeling is an effective tool for studying TMS systems and selecting stimulation parameters for more selective target engagement. Prior modeling efforts focused on calculating the spatial distribution of the E-field induced by transcranial magnetic stimulation in head models derived from magnetic resonance imaging data, typically using the finite element method [11].

As [12] mentioned the net TMS E-field is made up of primary and secondary components and the primary component, the E-field directly induced by the coil, can be calculated using scalar and vector potentials based on the geometric properties of the TMS coil. Due to induced charges on tissue interfaces, the secondary component can be found using the BEM, FEM, or FDM.

The research done by [3] they have created a quick computational auxiliary dipole technique (ADM) to determine the ideal coil position and orientation in order to increase TMS accuracy. The ideal coil placement maximizes the E-field in the targeted ROI in a specific direction or, conversely, the overall size of the E-field.

The most common computational methods used in the transcranial magnetic stimulation model design for the calculation of electromagnetic field distributions are the finite element method, boundary element method, finite difference method, and the current new proposed fast multipole boundary methods.

The computational approaches described above differ in terms of computational speed and spatial precision. Among them, the boundary method is fast as compared to the other finite element method and finite difference method. The issue with BEM, FEM, and FDM is that they offer a compromise between spatial accuracy and computational speed [12].

For this thesis, we apply and use a new TMS modeling method based on the combination of the boundary element method and the fast multipole method (BEM-FMM), which provides both speed and accuracy. As compared to the standard boundary element method and the finite element method used in SimNIBS or commercial FEM software ANSYS

Maxwell 3D, the BEM-FMM approach demonstrated faster computational speed (10-1000 times faster) [12] and superior accuracy for high-resolution head models and also for this approach the current study introduces an open-source software package for modeling TMS fields at high resolution using BEM-FMM.

Other related work on the TMS design is reviewed and summarized in the table next page in addition to the works already listed above.

Table 1: Summarized related works on the design of TMS computational model

	Previous works	Methods	Strength	Limitation
1.	P. Rastogi et.al, Transcranial Magnetic Stimulation-coil design with improved focality.	Calculation of the electric field (E-field) and modeling of TMS coils was performed using SEMCAD X.	Novel coil design QBC is proposed	Future research might make use of magnetic shielding and improvements to coils to increase size/angle and the QBC's focal point.
2.	Truong, Dennis Quangvinh, "Translational Modeling of Non-Invasive Electrical Stimulation [22]	Finite element method for a computational model of current flow and distribution	It uses more than 5 MRI images based on their body mass index	They did not sample the underweight BMI spectrum and it is TDCS work
3.	Fast computational optimization of TMS coil placement for individualized electric field targeting.	Auxiliary dipole method (ADM) for determining the optimum coil position and orientation	ADM can assess E-field uncertainty resulting from the precision limitations of TMS coil placement protocols.	The optimal coil orientation is ambiguous for ROIs containing highly curved sulcal walls.
4.	Timothy Wagner et. al, Noninvasive Human Brain Stimulation [2].	Finite element method for computational model	Design both the electrical and magnetic simulations	Need machine pules improvement
5.	Guidetti, M et.al, Neuroprotection and Non-Invasive Brain Stimulation: Facts or Fiction, 2022 [19]	Finite element method for computational method	They doing using the invitro animal model.	animal models do not completely fit with the complexity of human behavior

Chapter Three

System Model and Design

3.1 Methodology of the work

This thesis section includes data collection methods to understand the prevalence of MDD in the community, the area and level of the brain affected by MDD, current MDD treatment approaches, and TMS-based treatment with fundamental design elements. It also describes computational models used to calculate the electrical and magnetic field distribution of the TMS coil using fundamental mathematical equations and brain tissue models, head modeling, over all TMS system model design, design result optimization, simulation, and evaluation techniques.

3.1.1 Data Collection

To understand the distribution rate or prevalence of MDD in the local community, as well as current treatment methods and challenges, we chose two hospitals near Bahir Dar that serve a large population and have psychiatric departments: Tibebe Ghion and Felege Hiwot hospitals. As a result, all numerical data related to depression disorder cases were gathered with the assistance of psychiatry professionals and support staff. After collecting all relevant data, its quality and completeness are analyzed. The prevalence, severity, and impact of depressive disorder in the local communities are analyzed using data from the above two health facilities. In this thesis, this data is not used as components or inputs to our TMS design, but rather to understand the burdens and prevalence rates of MDD in our local communities.

3.1.2 Level and location of neural activity loss during MDD

Major depressive disorder is a serious medical condition that causes significant morbidity and disability. This thesis reviewed evidence from neuroimaging, neuropsychiatric, and brain stimulation experiments to answer the question of the location and leveling of neural activities in the brain during the depression. After reviewing the loss level which include decreasing the metabolic activities, dimensioned the neuron transmitter, altered brain connectivity and identify the location of neural activities in the brain during the depression, develop non-invasive transcranial brain stimulation system model for depression treatment.

3.2 Brain regions associated with Depression

MDD is distinguished by persistent poor mood, which is frequently accompanied by cognitive dysfunction, somatic symptoms, and decreased social function [4],[25],[26]. In several research, neuroimaging technologies, particularly magnetic resonance imaging, have been used to detect disorder-related patterns of brain alterations related with MDD. Researchers commonly use magnetic resonance imaging scan sequences such as high resolution structural imaging, which shows gray matter thickness in volume and brain morphology; diffusion tensor imaging, which depicts white matter microstructure; and functional magnetic resonance imaging, which depicts neuronal activity in target brain regions [4], [27], [31]. Anatomical MRI investigations have revealed several regional gray matter alterations in the frontal lobe, parietal lobe, thalamus, caudate, pallidum, putamen, and temporal lobes (For instance the hippocampus and amygdala) [4],[31]. White matter abnormalities, such as decreased fractional anisotropy in the cingulum, hippocampus, parietal areas, inferior temporal gyrus, and superior frontal gyrus, have been observed in diffusion tensor imaging investigations [31], [32]. Various regions of the brain communicate with one another, eventually forming complex brain networks.

According to the evidence from neuroimaging, neuropsychiatric, and brain stimulation experiments the following structure of the brain are mostly affected by MDD [1], [2], [5].

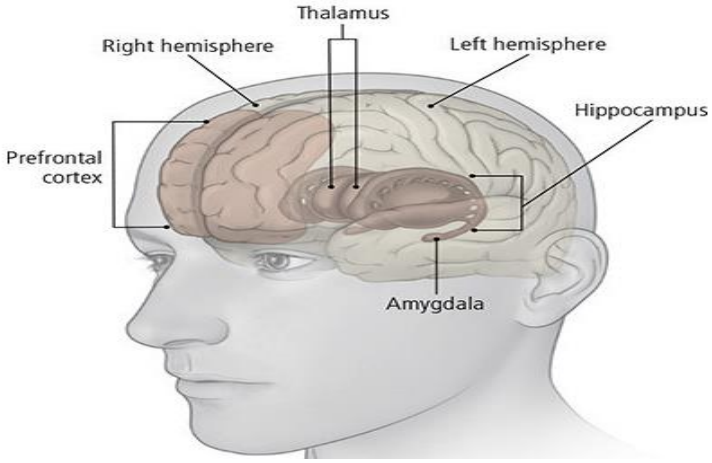

Figure 2: Region of the brain which is affected by MDD

3.2.1 Frontal Lobe

The most common site for showing anatomic abnormalities in MDD has been considered to be the change in volume of frontal regions [1],[2]. From the structure of frontal lobe the

anterior cingulate cortex (ACC) is anatomically connected to the dorsal neocortical and ventral paralimbic regions and is involved in cognitive and mood control processes [1],[3]. According to an functional magnetic resonance study [1],[3] the ACC has enhanced functional correlations with the dorsolateral prefrontal cortex (DLPFC) and the amygdala in MDD patients, implying that the ACC functions as a bridge between the DLPFC and the amygdala and is important in attention and emotion. The DLPFC is important for emotional, motivational, attentional, and executive functioning [4],[27]. Grey matter volume deficits in the DLPFC have also been identified in MDD patients compared to healthy controls [7], [22]. Brain activity in the DLPFC was also shown to be diminished, but it could be restored to normal after antidepressant medication [7],[31].

3.2.2 Amygdala

The amygdala is one of many deep brain structures linked to emotions, and activity in this region is increased when a person is sad or clinically depressed [5].

3.2.3 Hippocampus

The hippocampus is connected to memory retrieval and the principles of reward, and depressed patients' hippocampuses are smaller than those of healthy controls [4]. A small hippocampus was more common in people with depression who were over 40, had severe or numerous episodes, or both [4], [7], [27], [36]. Depressive patients had lower hippocampal brain activity, according to and functional magnetic resonance imaging study and also reduced grey matter volume and functional activity in the hippocampus would result in unpleasant feeling and the inability to process cognitive information in depressive patients [4].

3.2.4 Thalamus

The thalamus is regarded as a complex sensory information node that regulates arousal, emotion, and memory. Additionally, thalamic dysfunction and structural changes might cause an amnestic syndrome due to deficits in identification and recollection [8], [31]. Patients with MDD have shown significant volume decreases and structural alterations in the left thalamus [4], [31], [32]. A recent meta-analysis supported the observation that MDD patients had less grey matter volume in their right thalamus [7], [31].

3.2.5 Pariental lobe

During conditioning, the parietal lobe is engaged in the organization, decision making, and prediction of rewards, which analyses outcomes for future response choices that are unpredictable [9]. MDD patients had increased cortical thickness in the left inferior parietal gyrus as compared to healthy controls, and morphometric correlation analysis revealed a positive caudate-cortical link in the bilateral superior parietal lobe [7].

3.3 Approaches for MDD Treatment

Medication and psychotherapy are the most well-known and effective therapies for the majority of persons suffering with depression globally. In addition, interviews performed at two extremely populated hospitals in Bahirdar City, Felege Hiwot and Tibebe Ghion, reveal that the current treatment modalities used include a combination of medicine and psychotherapy. Antidepressants, such as selective serotonin reuptake inhibitors and serotonin-norepinephrine reuptake inhibitors, are often prescribed, and cognitive-behavioral therapy and interpersonal therapy are both forms of psychotherapy.

Despite the availability of effective medications, treating MDD in Ethiopia poses a number of challenges. These include a shortage of mental health specialists, limited access to mental health therapies, antidepressant side effects, a lack of therapy equipment, the expensive cost of antidepressants and their lower efficacy, the long recovery time, a lack of psychiatric service in small-level health facilities, and the stigma associated with mental illness. For patients with MDD who haven't responded or do not get better with antidepressants and psychotherapy, the other recommended procedure for treatment is brain stimulation therapy, which includes electroconvulsive therapy and involves passing electrical currents through the brain to influence the function and effect of neurotransmitters in the brain to alleviate depression, whereas TMS uses a treatment coil placed against the scalp to send brief magnetic pulses to stimulate nerve cells in the brain that are involved in mood regulation and depression.

3.3.1 TMS Based MDD Treatment

TMS is a non-invasive treatment in which magnetic fields stimulate nerve cells in the brain. It is a safe and effective technique to treat a variety of mental and physical health problems, including depression. TMS involves putting an electromagnetic coil on a patient scalp near the forehead and delivering short magnetic pulses painlessly into a region of the brain that

regulates mood or brain areas under depression. Figure 3 demonstrate that the representation of placement and working principles of TMS on the brain to treat the MDD.

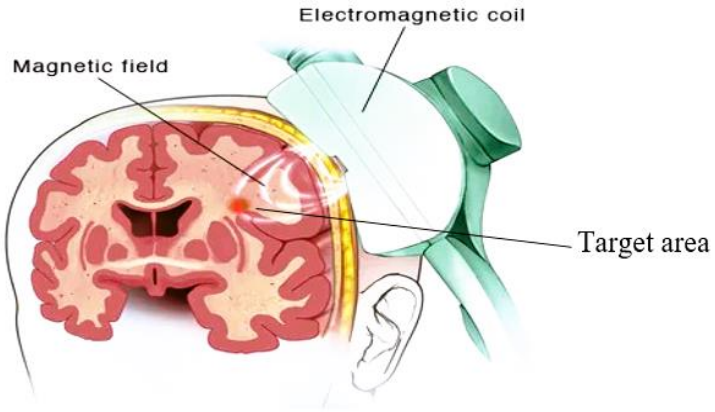

Figure 3: Sample TMS coil placement to treat the MDD

3.4 Computational Models of TMS

To investigate the distribution effect of the electromagnetic field features, we implement a mathematical computational model simulation of the magnetic coil on brain tissue using Matlab software packages. A magnetic coil is used in the noninvasive procedure known as TMS, which modulates the electrical activity of our brain. TMS computational modeling involves a compromise between computational speed and spatial precision. We used multiple software toolkits for good resolution TMS modelling in this investigation, and the different matlab and other software (like SimNIBS to allow simple, subject-specific operation) compatible toolkits included different computational approaches, including the newly developed BEM-FMM, which gives optimum solution computations near tissue interfaces. The BEM-FMM TMS modeling Toolkit is an application designed to simulate the electric fields produced by TMS. It uses BEM-FMM to obtain great accuracy and precision in electric field computations. To improve the accuracy of TMS, BEM-FMM is better to determining the optimum coil position and orientation. The best coil placement optimizes the E-field in the intended ROI either overall or along a predetermined direction [3]. Basic matlab computational scripts that develop coil/head position, perform computations, and output electric fields on surfaces and in volume are also required to construct TMS computational models. In addition to the basic scripts, it needs that head models withs in different brain compartments, the coil wire construction and CAD models,

coil testing, mathematical computation scripts which include the BEM-FMM, and the tissue conductivity values come from the SimNIBS TMS software package, which also used.

In this thesis, we also use multi mesh scripts to produce a combined mesh for the head model, tissue meshes, and to combine the different meshes into a single mesh. The basic set consists of stereolithography files in the shape of faceted shells for each unique brain region. Triangular facets with normal vectors pointing away from the shell are used in stereolithography files. The segmentation pipeline for SimNIBS and other pertinent software produce this as their default output.

3.5 Mathematical Model and Governing Equations

Maxwell's fourth rule of ampere's circuit law is used to generate fields by sending a large amplitude current pulse to the coil. Where the charge carrier distribution in the closed-loop coil generates a magnetic field perpendicular to the coil surface, the changing magnetic field causes an electric field in the conductive brain tissue medium. The differential equations used for expressing the above senecios, where J and Je represents the current density vector and externally generated current density respectively. H and A represent the magnetic field vector and potential, respectively, whereas B represents the magnetic intensity vector. Furthermore, the strength of the total induced electric field E of the coil is the sum of primary electric field which expressed in terms of magnetic vector potential $\mathrm{Ep} = -\mathrm{j}\omega\mathrm{A}$ and secondary electric field which expressed in terms of electric potential $\mathrm{Es} = -\nabla\emptyset$ and D the displacement vector.

$$J = \nabla \mathrm{X}\, \mathrm{H} = \sigma\mathrm{E} + \mathrm{j}\omega\mathrm{D} + \mathrm{Je} \tag{3.1}$$

$$\mathrm{E} = -\nabla\emptyset - \mathrm{j}\omega\mathrm{A} \tag{3.2}$$

$$\mathrm{B} = \nabla\mathrm{XA} \tag{3.3}$$

$$\mathrm{D} = \varepsilon\, \varepsilon\mathrm{r}\, \mathrm{E} \tag{3.4}$$

Where: ε, vacuum permittivity, $\varepsilon\mathrm{r}$, relative permittivity of the materials which is the ratio of permittivity of dielectric material to permittivity of vacuum, σ conductivity of the human brain layers, ∇ vector operator expressed as $\nabla = i\frac{\partial}{\partial x} + j\frac{\partial}{\partial y} + k\frac{\partial}{\partial z}$, ω is angular frequncy which is expressed as $\omega = 2\pi f$, and $\emptyset$ is the electric potential, in the node it is calculated by solving the Laplace equation $\boldsymbol{\nabla} \cdot (\boldsymbol{\sigma}\boldsymbol{\nabla}\emptyset) = 0$.

The behavior of electric fields inside a volume conductor, such as the human head, is governed by differential equations like equations 3.1 to 3.6 and boundary integral equations such as equation 3.7, which are used to reduce computation time and increase accuracy when calculating the distribution of electric and magnetic fields on the conducting medium, such as human brain tissue.

At the typical frequencies used in TMS (~10 kHz), electric fields can be well described using a quasi-static approximation, which leads to a Poisson equation [18].

$$\boldsymbol{\nabla} \cdot (\boldsymbol{\sigma}\boldsymbol{\nabla}\emptyset) = -\nabla . \sigma \frac{\partial A}{\partial t} \tag{3.5}$$

with the Neumann boundary conditions

$$\frac{\partial \emptyset}{\partial \cap} = -\cap . \frac{\partial A}{\partial t} \; on \; \partial\Omega \tag{3.6}$$

where, A is a magnetic vector potential. This quantity is defined such that B = $\boldsymbol{\nabla}$ **x A**, where B is the magnetic field produced by the coil. The spatial distribution of a coil magnetic field B(p) depends on its geometric properties such as shape, number of turns, and radii [15].

3.5.1 Fast Multipole Method (FMM)

The FMM is a frontal program compiled for MATLAB and the FMM algorithm's tolerance level is set to 0 or 1 (the relative least-squares error is guaranteed not to exceed 0.5% or 0.05%, respectively) [12]. With this FMM version, it is simple to include and accurately assess a limited number of analytical neighbor integrals on triangular patches. The FMM can be used to severalfold accelerate boundary integral equations solutions to reduce CPU time in an FMM-accelerated BEM and also the fast multipole method used in solving of important BEM system of equations in engineering problems [16].

3.5.2 Boundary element method (BEM)

The boundary element method is a numerical method for resolving boundary-value or initial-value problems that are expressed using boundary integral equations. The FDM, FEM, and element free method are domain-based mathematical methods that use ordinary differential equation or partial differential equation formulations like the equations expressed in 3.1 to 3.6, whereas the BEM and boundary node method are boundary-based methods that use BIE formulations [16]. Particularly with the aid of the FMM, the BEM has gained a great deal of interest in the field of computational mechanics. The BEM's applications now cover a broad range of engineering disciplines and go well beyond the

scope of traditional potential and elasticity theories, including wave propagation (acoustic, elastic and electromagnetic), design sensitivities, and optimizations [7], [16]. In this study we use the direct charge-based boundary element approach in a conducting medium. When an external electromagnetic stimulus (a primary electric field $\boldsymbol{Ep}(\boldsymbol{r})$, either conservative or solenoidal) is delivered, induced charges with a surface charge density $\rho(\boldsymbol{r})$ in C/m2 occur on tissue conductivity interfaces (S). The induced surface charges change (usually block and/or redirect) the primary stimulus field. Coulomb's law governs the total electric field in space, with the exception of charged interfaces [7]. The appropriate integral equation is found by putting the total electric field Et in a form that takes into account the primary solenoidal field Ep as well as a conservative contribution from the secondary induced surface charge density Es, which is represented as [13], [17], [18]:

$$\mathrm{Et(r)} = \mathrm{Ep(r)} + \mathrm{Es(r)}, \quad Es(\mathrm{r}) = \int_S \frac{1}{4\pi\varepsilon o}\frac{\mathrm{r}-\mathrm{r}'}{|\mathrm{r}-\mathrm{r}'|^3}\rho(\mathrm{r}')\mathrm{d}r' \ , \ \boldsymbol{r} \notin S \tag{3.7}$$

where εo is the permittivity of vacuum, $\boldsymbol{r}$ approaches surface S from both sides (inside and outside) and the electric field is discontinuous at the interfaces. When approaching a charged interface (S) with a normal vector ($\boldsymbol{n}$) from either direction (inside or outside), the electric field is given by:

$$Ein/out = Ep(\mathrm{r}) + \int_S \frac{1}{4\pi\varepsilon o}\frac{\mathrm{r}-\mathrm{r}'}{|\mathrm{r}-\mathrm{r}'|^3}\rho(\mathrm{r}')\mathrm{d}r' \pm n(r)\frac{\rho(\mathrm{r}')}{2\varepsilon o} \ , \boldsymbol{r} \in S \tag{3.8}$$

An integral equation for $\rho(\boldsymbol{r})$, which is the Fredholm equation of the second kind, is obtained after substitution of equation (3.8) into the quasistatic boundary condition, which enforces the continuity of the normal current component across the interface, that is

$$\sigma in\, \boldsymbol{n}(\boldsymbol{r}) \cdot \boldsymbol{E}in = \sigma out\, \boldsymbol{n}(\boldsymbol{r}) \cdot \boldsymbol{E}out, \boldsymbol{r} \in S \tag{3.9}$$

The results are looks like the equation below:

$$\frac{\rho(\mathrm{r})}{2} - \frac{\sigma\mathrm{in}-\sigma\mathrm{out}}{\sigma\mathrm{in}+\sigma\mathrm{out}}\mathrm{n(r)}.\int_S \frac{1}{4\pi\varepsilon o}\frac{\mathrm{r}-\mathrm{r}'}{|\mathrm{r}-\mathrm{r}'|^3}\rho(\mathrm{r}')\mathrm{d}r' = \frac{\sigma\mathrm{in}-\sigma\mathrm{out}}{\rho\mathrm{in}+\rho\mathrm{out}}\mathrm{n(r)}\,.\varepsilon\mathrm{oEp(r)} \ , \boldsymbol{r} \in S \tag{3.10}$$

where $\boldsymbol{n}(\boldsymbol{r})$ is the outer normal vector to the particular boundary and $\sigma in/out$ are the two distinct tissue conductivity values on either side of the boundary. The first (simpler) task of the numerical solution is to compute the excitation – the primary electric field $\boldsymbol{Ep}(\boldsymbol{r})$ – everywhere at tissue conductivity boundaries in equation (3.10). The second (more

complicated) task is to compute the induced charge density by solving integral equation (3.10) of the second kind iteratively and thus compute the secondary electric field $\boldsymbol{Es}$.

3.6 Computation of primary Electric and Magnetic fields:

Primary electric and magnetic fields $\boldsymbol{Ep}$ and $\boldsymbol{Bp}$ of a TMS coil are computed using FMM. The number of elementary current filaments is ultimately unlimited. Consider a small straight element of current $ij(t)$ with segment vector $\boldsymbol{sj}$ and center $\boldsymbol{pj}$. Its magnetic vector potential, $\boldsymbol{Ap}$, at an observation point $\boldsymbol{ci}$ is given by

$$\mathrm{Ap(ci,t)} = \frac{\mu o}{4\pi}\frac{\mathrm{ij(t)\ Sj}}{|\mathrm{Ci-pj}|} \tag{3.11}$$

where $\mu 0$ is magnetic permeability of vacuum and index p again means the primary field. The electric field generated by this current element is

$$\mathrm{Ep} = -\frac{\partial \mathrm{Ap}}{\partial \mathrm{t}} \tag{3.12}$$

Assuming harmonic excitation with angular frequency ω and omitting the redundant phase factor of $-j$, one has

$$\mathrm{Ep} = \frac{\mu o \omega}{4\pi}\frac{\mathrm{ioj\ Sj}}{|\mathrm{Ci-pj}|} \tag{3.13}$$

Now consider multiple straight short current segments with moments $ij0\boldsymbol{sj}$ forming the coil. Also consider multiple observation points $\boldsymbol{ci}$ which coincide, for example, with triangle centroids of the head surface mesh. For every observation point, the electric field in equation (3.13) is computed via FMM as a potential of a single layer repeated three times, i.e., separately for each component of the field.

The same element of current generates a magnetic field $\boldsymbol{Bp}$ given by Biot-Savart law

$$\mathrm{Bp} = \frac{\mu o}{4\pi}\frac{\mathrm{ioj\ Sj\ x(Ci-Pj)}}{|\mathrm{Ci-pj}|\text{^}3} \tag{3.14}$$

3.7 Computation of secondary Electric field:

The fast multipole method speeds up computation of a matrix-vector product by many orders of magnitude. In the present problem, such a matrix-vector product appears when an electric field from many point sources $\rho(\boldsymbol{r'})$ in space has to be computed at many observation points $\boldsymbol{r}$. Namely, discretization of the surface integral in equation (3.7) or

equation (3.10) and use of the zeroth-order piecewise constant basis functions (pulse bases) yields

$$\boldsymbol{Es}(\boldsymbol{ci}) = \sum_{\mathrm{j=1}}^{\mathrm{N}} \frac{\mathrm{Aj}\ \rho\mathrm{j}}{4\pi\varepsilon\mathrm{o}} \frac{(\mathrm{Ci}-\mathrm{Cj})}{|\mathrm{Ci}-\mathrm{Cj}|\hat{}3} \tag{3.15}$$

where Ai, $\boldsymbol{ci}$, i = 1, …, N are the areas and centers of triangular surface facets ti; ρi are triangle surface charge densities in C/m2, and $Aj\rho j$ are elementary charges located at $\mathbf{c}j$. Equation (3.15) is straightforwardly computed via the same FMM library, as an electric field of a given charge distribution. Such a computation is done at every step of an iterative solution for integral equation (3.9)

3.8 Computing normal Electric field at the interface

Equation (3.8) can be multiplied by the surface normal vector $\boldsymbol{n}$ to obtain the normal electric field inside the surface ($\boldsymbol{n} \cdot \boldsymbol{E}in(\boldsymbol{r})$, the normal electric field outside the surface ($\boldsymbol{n} \cdot \boldsymbol{E}out(\boldsymbol{r})$, and the normal field discontinuity for any conducting interface ($d\boldsymbol{n} \cdot \boldsymbol{E}$). All three quantities are in direct proportion to one another. For any observation point $\boldsymbol{r} \in S$ and any conducting interface S.

$$n.Ein(r) = \frac{\sigma\mathrm{out}}{\sigma\mathrm{in}-\sigma\mathrm{out}} \frac{\rho(\mathrm{r})}{\varepsilon\mathrm{o}}\ ,\ n.Eout(r) = \frac{\sigma\mathrm{in}}{\sigma\mathrm{in}-\sigma\mathrm{out}} \frac{\rho(\mathrm{r})}{\varepsilon\mathrm{o}}\ ,\ \mathrm{dn.E} = \frac{\rho(\mathrm{r})}{\varepsilon\mathrm{o}} \tag{3.16}$$

The normal component of the total E-field at the inside/outside conductivity boundaries is clearly dependent on the induced surface charge density.

3.9 Head Modeling

To effectively capture volume conduction effects, personalized head models with segmented brain white matter (WM), brain gray matter (GM), Cerebrospinal fluid (CSF), skull, and scalp are required. Since magnetic resonance imaging scans don't emit ionizing radiation, don't require contrast agents, and provide a fair contrast between soft tissues, they are frequently used as the basis for these segmentations [15]. However, manually segmenting magnetic resonance images requires several hours of labor for just one patient, making it a time-consuming operation. Several head modeling solutions for TMS have been suggested throughout the years in an attempt to automate this procedure. One of these tools, which is included in the SimNIBS package, makes use of the brain segmentation techniques used by FreeSurfer [15]. SimNIBS is a popular software application for modeling TMS and can generate individualized head models automatically from magnetic

resonance images, simulate electric fields using mathematical computational methods and perform various postprocessing operations [17].

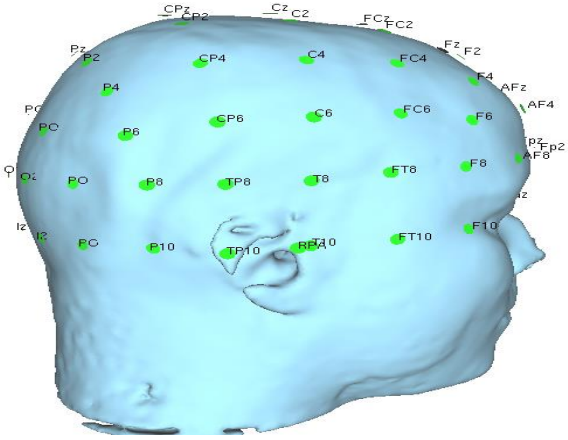

Figure 4: SimNIBS 3D head model simulation outputs with its different coil position

The data for each brain compartments is generating using simNIBS software pipe lines. Design the brain compartments (Skin, Skull, CSF, GM, and WM) from the magnetic resonance image segmentation. Which is also generate the matlab compatible images and scripts from the MRI impute image.

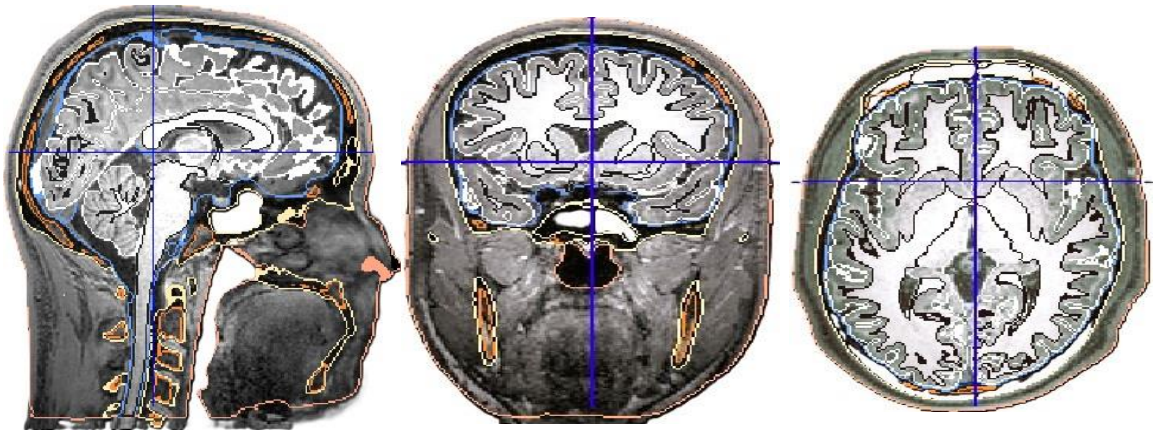

a b c

Figure 5: SimNIBS MRI image segmentation simulation out puts

Figure 5 above demonstrate that the image segmentation outputs of the simNIBS using the input T1 weighted MRI image (a) the automated image segmentation on x coordinate plane, (b) y coordinate plane and (c) on the z coordinate plane. To develop and analyze the computational models of the head, we have to create and analysis all basic brain compartments (skin, skull, CSF, GM, and WM).

The scalp, skull, cerebrospinal fluid, gray matter, and white matter are the five unique anatomical layers of the human head.

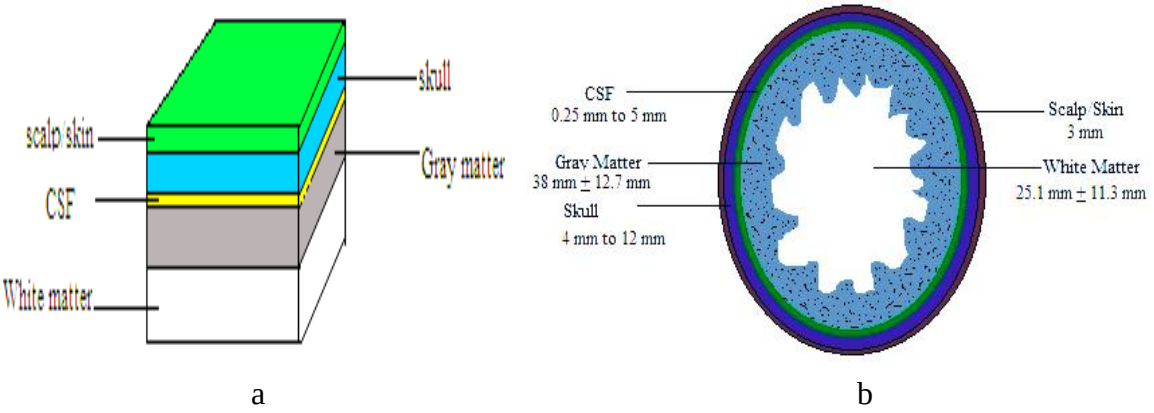

a b

Figure 6: Cross sectional model of the Brain compartments

Figure 6 above illustrate that different layer design of the brain compartments which is (a) 3D Cross sectional views model includes basic layers and (b) five layers cross sectional spherical model with each layer average thickness of human brain.

For high-resolution head models, the quasistatic BEM-FMM modeling approach is a computational tool for obtaining an accurate electric and magnetic field solution.

3.10 Optimization of the Design results

TMS is a non-invasive brain stimulation technology that use magnetic pulses to modulate neuronal activity. Optimizing the orientation and position of the TMS coil is critical for achieving therapeutic benefits. The researchers used different computational algorithms to optimize TMS coil placement. These algorithms take into account the target brain region, individual head anatomy, and desired stimulation intensity.

For the transcranial magnetic neurostimulation modality, simulating the electric fields within a patient-specific head model is the primary and often only way to foster spatial targeting and obtain a quantitative measure of the required stimulation dose [16]. The modeling of quasi-static electromagnetic fields in biological tissues can be accomplished primarily through the use of computational methods [12],[15],[18].

Transcranial magnetic stimulation computational modeling involves a trade-off between computational speed and spatial accuracy. In this study, we use a software toolkit for high-resolution TMS modeling, which may provide the best of both computational speed and spatial accuracy. The toolkit makes use of the newly developed boundary element fast

multipole method (BEM-FMM), which provides accurate solution computations close tissue interfaces and it is designed for a large, medically-oriented computational research community and runs on the matlab platform [12],[19],[20].

3.11 Simulation and results analysis

The magnetic field estimations in the regions of interest are only one example of the kind of useful information that simulations provide to TMS trainers. Numerous open-source software initiatives were created to make TMS simulation more accessible. Some of the open-source software are:- a new MATLAB package for BEM-FMM-based TMS simulations that was made in 2019 available, SimNIBS, which includes TMS and a head segmentation pipeline called mri2mesh, was published in 2013 [15] and it has recently been enhanced to incorporate TMS optimization, as well as a new head segmentation process known as headreco and others open-source are available. For this study, we use the aforementioned open-source software package for computational modeling simulation and analysis.

3.12 Evaluation of the design simulation

The outcome of the simulation methodologies and techniques are described and analyzed after the modeling of the human brain and coil.

The general frameworks of TMS design and simulations are shown in the diagram below.

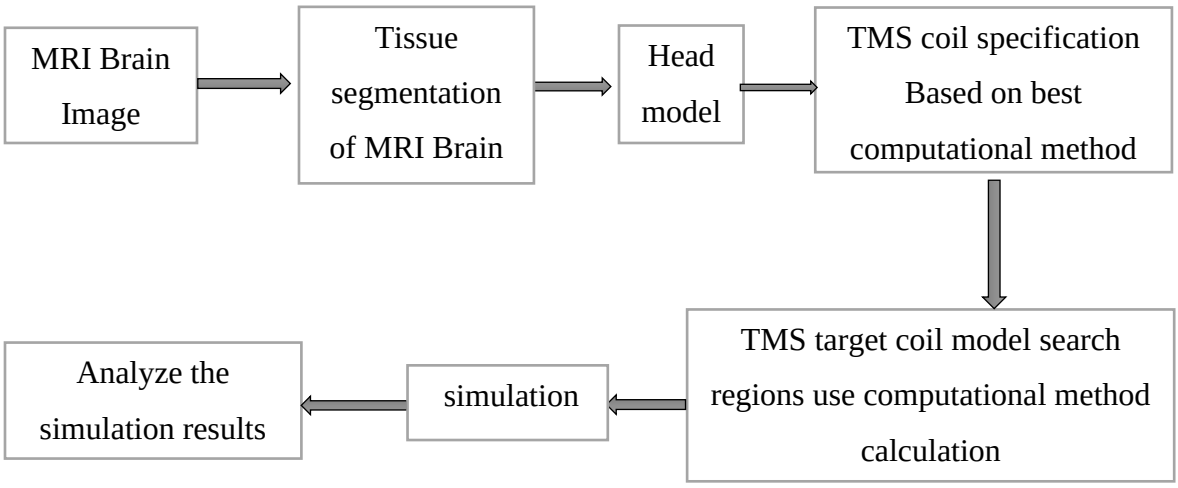

Figure 7: Methodology of TMS computational design and simulations

3.13 Over all TMS system Model Design

TMS systems used for therapeutic purposes consist of several fundamental components, including a magnetic coil, which generates magnetic fields that induce electric currents in the brain, a simulator, a control unit, and positioning system. As a result, in this thesis, we design, simulate, and analyze basic TMS components, beginning with the development of a human head model. To create the human head model, we use an MRI brain image as input in SimNIBS software, which can autonomously generate brain tissue segmentation and individual meshes. After creating the separate meshes, we integrated them to generate single human head models with particular TMS coil placement positions, as shown in figure 5. After developing the head model, we created the figure-eight type TMS coil model with basic input parameters such as the coil's radius of 0.02 M, thickness of 0.01 M, sample testing current of 1A, and also by writing different matlab scripts we create various planners ranging TMS coils from single ring to double planner figure-eight type, which generate both the CAD and mesh of the TMS coil. We used EEG and MRI based guidance for exact coil placement to examine each brain coil position which are affected by MDD and also by using the SimNIBS and matlab software we generate each brain compartment's structure. To generate each compartment of the human brain we write the mat lab scripts that display a mesh from a *.mat file. After we create and generate the brain tissue compartment and understand the exact position of brain which affected by MDD we are going to correctly positioning the TMS coils on the brain compartments and analysis the electromagnetic fields by applying sample current and constant input parameters which includes coil steady state or the sample current to calculate magnetic field I0= 5e3 A, define each precise coil position, define the sample field margin(the boundary line or the area immediately inside the boundary) is 0.8, define coil time varying current dI/dt=9.4e7 Amperes/sec to find the electric field, vacuum permittivity, conductivity of each brain compartments (according to lists in table 6 in chapter 4) and define the observation line. To simulate and analyze the TMS coil electromagnetic field distribution on the brain tissue layers, we employed or proposed for this thesis the BEM-FMM computational model, which improved accuracy, reduced CPU time, and increased precision as compared to the other computational methods like FEM, FDM, ADM and others. We used the BEM-FMM computational mathematical model which is compatible to the matlab software to calculate

the electric field distribution in each brain compartment as well as the magnitude of the magnetic field in each brain compartment based on the mathematical equation model listed from (3.7) to (3.16). We also calculate and analyze the charge density, Lorentz force, and electric potentials. We also used an electric and magnetic coil tester line to assess the performance of the planned or intended TMS coil. Lastly, but not least, we calculated and analyzed the magnitude of magnetic and electric field distribution of the designed TMS coil in different cross- sectional planes.

In general, the TMS model system for depression treatment with its basic components is show in the figure 8 below: a stimulator or electric circuit components or electric source, coil system, and targeting tissue or brain compartments. The stimulator generates a high electrical current that flows through the coil. This generates a rapidly changing magnetic field that penetrates the scalp and skull, producing electrical currents in the targeted brain region.

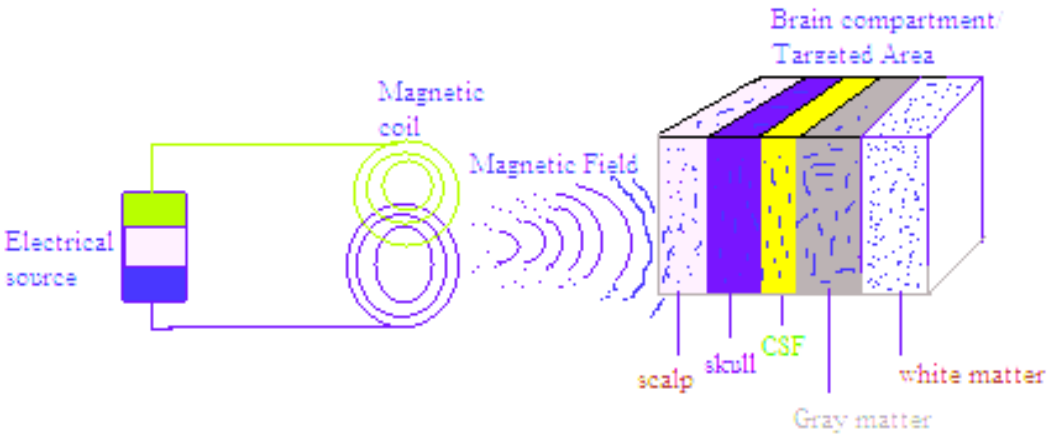

Figure 8: Overall system model of the TMS brain stimulation

Chapter Four

Results and Discussions

4.1 Data Collection to Analysis the prevalence of MDD

4.1.1 Prevalence of Major Depressive Disorder in the local community

Due to the availability of psychiatry departments, Tibebe Ghion and Felege Hiwot, two highly populated community service provider specialized hospitals, were chosen for this research work. To assess the total number of psychiatric patients' data from these two hospitals, first the legal and ethical-related issues were approved in collaboration with Bahir Dar University's faculty of electrical and computer engineering. As a result, all data related to all psychiatric disorder and specifically major depression disorder cases were gathered with the assistance of psychiatry professionals and support staff. The data related to all psychiatric disorders and major depression collected from the two hospitals is shown below.

4.1.1.1 Data from Felege Hiwot Hospital

From the hospital, there is one primary psychiatric department or ward with a total of 17 beds, and according to the data recorded in the patient registration book, they serve more than 20,000 new and repeat patients each year. And also, according to the hospital's national disease classification and reports, they provide treatment for more than 20 psychiatric disorder diseases, which are listed below.

Table 2: A list of the mental health disorders treated in Felege Hiwot Hospital

National Disease classification		National Disease classification
Schizophernia		Poisoning or suicide
Bipolar Disorder		Schizophernia Letonset
Psychosis (acute& transient)		Pain (Somatization) disorder
Major depressive episode		Dementia with psychosis
psychosis unspecified		Developmental delay
Generalized anxiety disorder		Sleep disorder
Dissociative (conversion) disorder		Headache unspecified
Autism (ADHD)		Personality disorder
Adjustment disorder		Petit mal or absence seizures

Drug withdrawal state		Status epilepticus
Premature Ejaculation		substance use disorder

The one-year new coming patient prevalence of major depression disorder data in Felege Hiwot hospital is looks like bellow (from July 2014 E C to June 2015 E C).

Table 3: The prevalence of MDD in Felege Hiwot Hospital, based on one-year new patient arrivals data

		Male				Female				
Month	Age range	< 1 yr-14 yrs	15-29 yrs	30-64 yrs	>=65 yrs	< 1 yr-14 yrs	15-29 yrs	30-64 yrs	>=65 yrs	Total
July		0	9	6		0	7	8	1	31
August		0	14	8		0	8	5	2	37
Sep.		0	4	2		0	6	5		17
Oct.		0	4	2	1	0	6	5	1	19
Nov.		0	1	1		0	2		2	6
Dec.		0	12	7		0	14	5		38
Juna.		0	11	8	1	0	14	8		42
Feb.		0	6	7	1	0	12	17	1	44
March		0	10	9	1	0	12	6	3	41
April		0	7	8		0	2	4		21
May		0	10	8	1	0	5	3	1	28
June		0	5	2	1	0	3	2		13
Total		0	93	68	6	0	91	68	11	337

The above level of MDD prevalence statistics for one year at Felege Hiwot hospital is shown in a bar and line graph below figure 9.

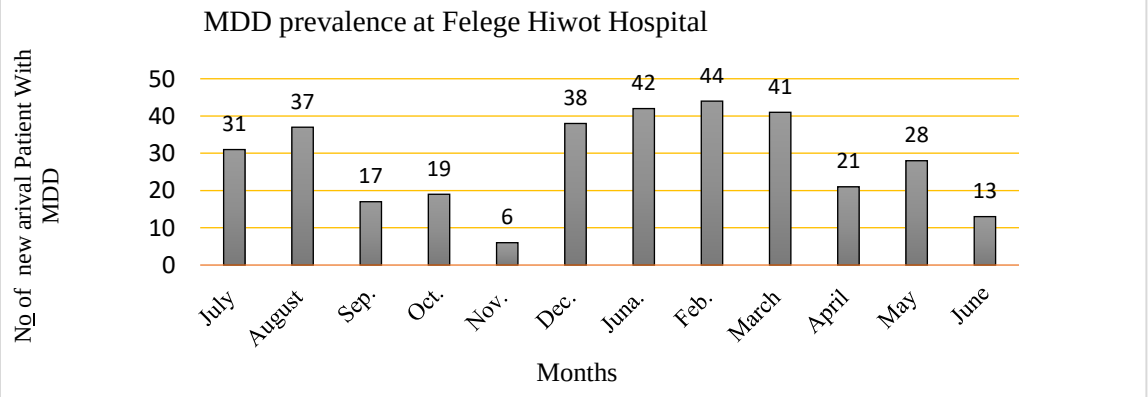

Figure 9: A bar graph show the prevalence of MDD in Felege Hiwot Hospital

According to the data which shows table 3 above, the total number of males who are under MDD with the age range of 15 to 29 years old are 93, which is 27.6% of the total case, from 30 to 64 years old are 68, which is 20.18% of the total case, above 65 years old are 6 which is 1.78% of the total case, from 1 to 14 no cases under MDD which is 0% of the total case, and the total number of females who are under MDD with the age range of 15 to 29 years old are 91 which is 27% of total case, from 30 to 64 years old are 68 which is 20.18% of the total case, above 65 year are 11 which is 3.26% of the total MDD patients.

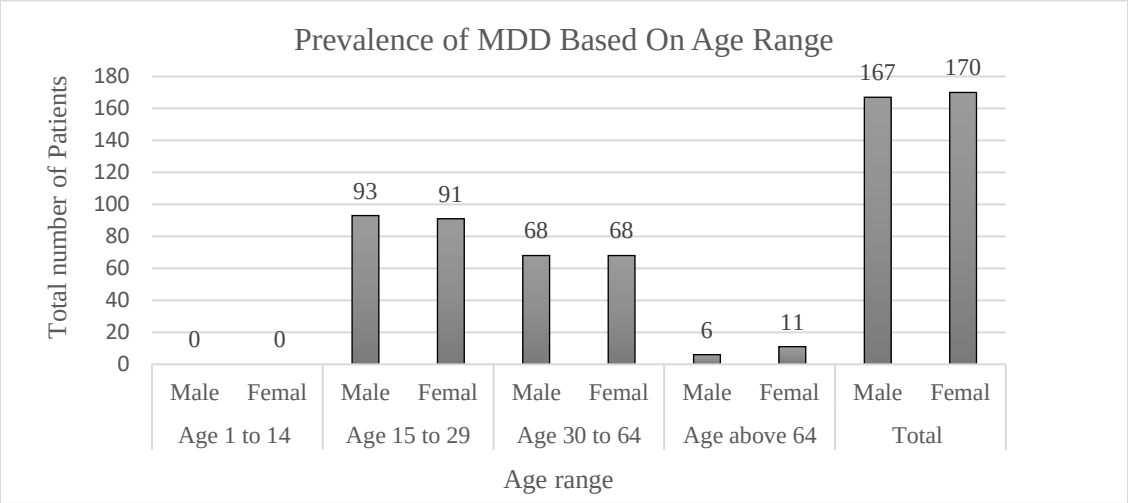

Figure 10: The prevalence of MDD in Felege Hiwot hospital based on age range

According to the data in the table 3 and figures 10 above, the prevalence of MDD is highest in people aged 15 to 29 years, both males and females, accounting for 54.6% of all cases; in people aged 30 to 64 years, both males and females account for 40.36% of all cases; and in people aged 64 and older, both males and females account for 5.04% of all cases.

Furthermore, analyses show that the total number of males with MDD is approximately 167, accounting for 49.555% of all patients, and the total number of females with MDD is approximately 170, accounting for 50.445% of all patients, demonstrating that females have a higher prevalence of MDD than males.

In addition, according to one-year hospital patient registration book statistics and the health management information system, they treat nearly 16,000 total mental patients, with approximately 23% (around 3,680) of these total patients suffering from MDD. Among the total number of 16,000 cases, around 9.8%, or 1,600, are new arrivals, with the remaining 90.8% being repeat patients.

4.1.1.2 Data from Tibebe Ghion Hospital

Tibebe Ghion Specialist Teaching Hospital is a well-known service provider that works collaboratively with Bahirdar University's clinical teaching disciplines in the College of Medicine and Health Sciences. According to the data registration sheet book and the health management information system report, 3174 new patients with mental illnesses were admitted to the facility between July 2014 EC and April 2015 EC, with 641 of them accounting for about 20.2% of total MDD cases.

Based on the data, the prevalence of MDD at Tibebe Ghion hospitals is shown in the table 4 below, categorized by age range.

Table 4: Ten-month data show the distribution of MDD at Tibebe Ghion hospital

Age range	Total number of males	Total number of females	Sum total
Age 1 to 14	5	10	15
Age 15 to 29	170	215	385
Age 30 to 64	90	103	193
Age above 64	23	25	48
Total	288	353	641

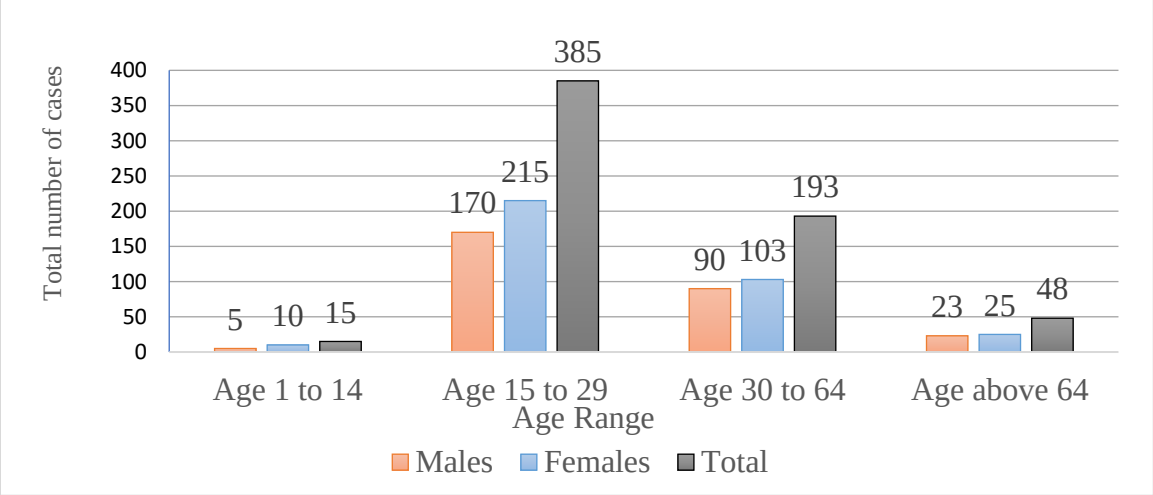

Figure 11: The distribution rate of MDD according to age range

According to the above data in table 4 and figure 11, the total number of cases and prevalence rate of MDD new arrival cases within ten months from age 15 to 29 are 385, which is 60.06% of the total cases; from age 30 to 64 are 193, which is 30.109% of the total cases; age above 64 are 48, which is 7.5% of the total cases; and age less than 15 are 15, which is 2.34% of the total cases. Furthermore, according to data from the hospital's

health management information system and patient data registration book sheet, the hospital provides a total number of psychiatric services around 25,000 patients each year, from this total number around 2.56% being only MDD new arrivals and the remainder, or around 14% which is around 3500 cases are other new arrival psychiatric cases and the remaining 83.44% which is around 20,860 cases are repeat patients. From these 20,860 total repeated cases around 5,215 which is 25% of the repeated cases are MDD.

The prevalence, severity, and impact of major depressive disorder in the local communities are analyzed using data from the above health facilities. From these hospitals totally in one year they provide service total number of psychiatric cases are around 41,000, among them around 4879 which is 11.9% of the total cases are new arrival psychiatric patients and around 937cases which is 19.204% of the total new arrival cases only MDD.

4.2 Simulation and Analysis of TMS based Brain Stimulation

The simulation and analysis of TMS-based brain stimulation need the use of computational models to predict TMS effects such as the distribution of magnetic and electric fields, charge density, and Lorentz force on human brain tissue layers. This section of the thesis explains the assumptions for the brain model, the basic parameters used to describe the TMS system, the coil model, and the analysis of the simulation findings.

4.2.1 Assumption on Brain Model

The brain is composed of interconnected modules that execute specialized functions. In this thesis, we assume that the brain has five main layers: scalp/skin, skull, cerebrospinal fluid, grey matter, and white matter. These layers have their own particular conductivities, thicknesses, permeability and biological structures. In addition, we apply the SimNIBS software-generated brain MRI matlab compatible image to analyze simulations of the basic electric and magnetic field distributions and charge density on each layer.

4.2.2 Simulation Parameters

The basic parameters for simulation and analysis of the TMS system model for understanding the computational model outputs on matlab like the electric and magnetic field distribution on brain tissue layers includes the thickness and conductivity of each brain layer, the input current for TMS coil and other quantities are reviewed and explain on this section of study.

4.2.2.1 Thickness of Brain tissue layers

Each layer of brain tissue has a particular average thickness. The table 5 below lists the average thickness of each layer of brain tissue based on research conducted by [12], [13], [14], and the neuroimaging studies in simNIBS software packages.

Table 5: Thickness of brain tissue compartment

Tissue type	Average Thickness(mm)
Scalp/Skin	3 mm
Skull	4 mm to 12 mm
Cerebrospinal fluid	0.25 mm to 5 mm
Gray matter	38 mm $\pm$ 12.7 mm
White matter	25.1 mm $\pm$ 11.3 mm

4.2.2.2 Conductivity of the Brain tissue layers

The majority of the compartments in the head models were thought to be electrically homogenous and isotropic [13]. According to the research conducted by [11], [14] and the neuroimaging studies in SimNIBS software packages the average conductivities of basic brain tissue layers are listed below in the table 6.

Table 6: The conductivity of basic brain tissue layers

Tissue type/Brain compartment	Electrical Conductivities of tissue layer(S/m)
Scalp/skin	0.465 S/m
Skull	0.025 S/m
Cerebrospinal fluid	1.654 S/m
Gray matter	0.275 S/m
White matter	0.126 S/m

4.2.3 Results analysis

4.2.3.1 Brain compartments

The human brain is divided into six fundamental compartments: the skin (the outermost layer), the scalp, cerebrospinal fluid, the gray mater, and the white mater (the most inner layers of the human brain structure). Each brain layer has unique electrical and magnetic distribution characteristics, as well as different conductivity properties for electric and

magnetic fields. Among these here below shows the gray and white matter brain compartment matlab simulation outputs.

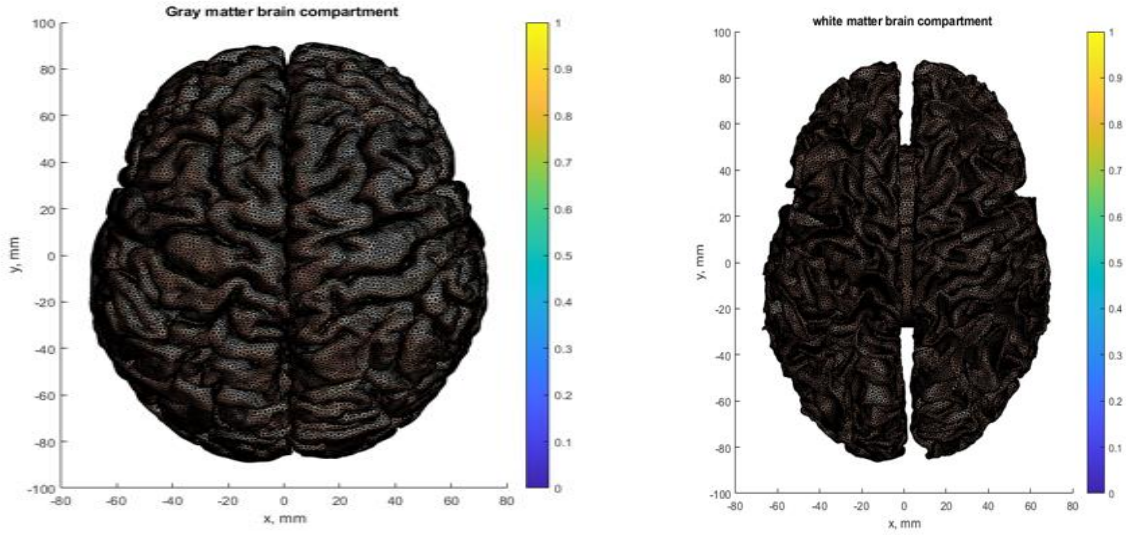

Figure 12: Simulation outputs of fundamental human brain compartment models.

Based on the defined Electrical conductivities and thickness of tissue and the governing maxwell questions the outputs of SimNIBS simulations of brain compartments are shown figure 13 below.

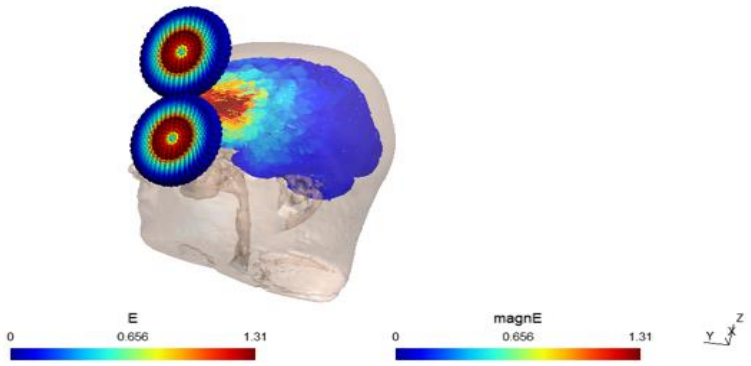

Figure 13: The simNIBS simulation of electric field distribution on gray matter

The simulation outputs from figure 13 illustrates that the distance between the coil and the brain tissue or skin is around 4mm, the conductivity of the grey matter is approximately 0.275 S/m, the charge distribution (dI/dt) is approximately 1.00x1e6 A/s, and there are three coordinate positions. And also, the simulation outputs show that the electric field distribution on the gray matter of brain tissue layer and its magnitude varies from 0 to 1.31V/m.

Generally, the figure 13 simulation summarized as: in table 7 gray matter field Percentiles, top percentiles of the field (or field magnitude for vector fields) and in table 8 field focality mesh volume or area with a field >= X% of the 99.9th percentile.

Table 7: GM brain simulation summary on simNIBS, Field magnitude

Field	99.9%	99.0%	95.0%
E	1.20e+00 V/m	7.80e-01 V/m	3.98e-01 V/m
MagnE	1.20e+00 V/m	7.80e-01 V/m	3.98e-01 V/m

Table 8: GM brain simulation on simNIBS, Field Focality mesh volume or area

Field	75%	50%
E	4.62e+03 mm^3	1.66e+04 mm^3
MagnE	4.62e+03 mm^3	1.66e+04 mm^3

Figure 14 below shows the distribution of electric field and current densities in human brain tissue layers at different TMS coil coordinate locations. The image depicts the distribution of the electric field at the scalp's brain layers with C5 electroencephalogram coordinate positions of x, y, and z (-77.5, 11.4, and 36.3), the coil-to-cortex distance is 4mm, and the current density of the sampled coil is 1.00x1e6 A/s. The simulated outputs of the electric field range from 0.00 V/m to a maximum of 39.37 V/m, as shown in the figure below.

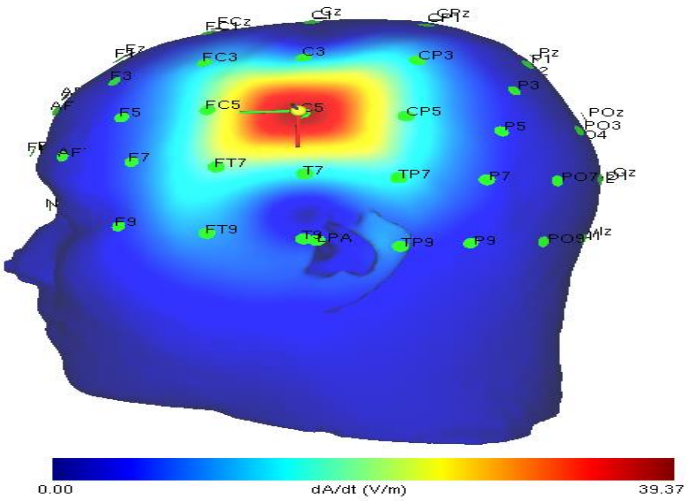

Figure 14: Electric field distribution SimNIBS simulation results the scalp

The figure 15 bellow depicts the distribution of the electric field at the brain layers of gray matter with CP1 electro encephalogram positions/coordinates of the TMS coil, which are x, y, and z (-35.5, -27.8, and 88.3), the distance between the source of the field and the current density, which is called coil to cortex distance 17.08mm from the gray matter, and the sample current density of 1.00x1e6 A/s. The electric field outputs range from 0.23 V/m to a maximum of 19.43 V/m, indicating that the electric field strength decreases from the outside layer (skin) to the interior brain layer (gray matter), as shown below.

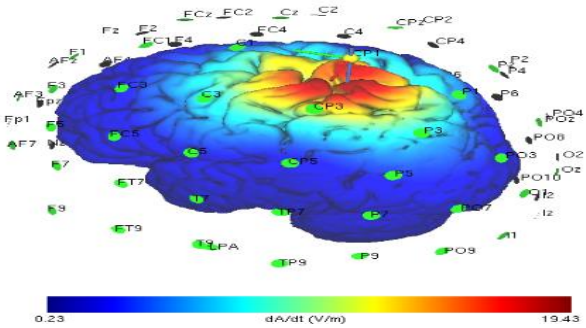

Figure 15: Electric field dispersion SimNIBS simulation output of gray matter

4.3 TMS magnetic coil model

A TMS magnetic coil model is a device used in neuroscience research and therapy to provide concentrated magnetic pulses to specific brain regions. The coil is often placed on the scalp and generates a magnetic field that can induce electrical currents in the brain, allowing researchers and physicians to study brain activity and potentially cure neurological and psychiatric conditions such as major depressive disorder. TMS coils are categorized into three basic types: figure-eight coils, circular coils, and H-coils, each with distinct features and applications.

For this thesis, we create and design figure-eight coil types with matlab scripts that can show both a CAD surface mesh and a computational wire grid for a ring with a total current of 1 A. Here, we design a single conductor in the shape of a ring.

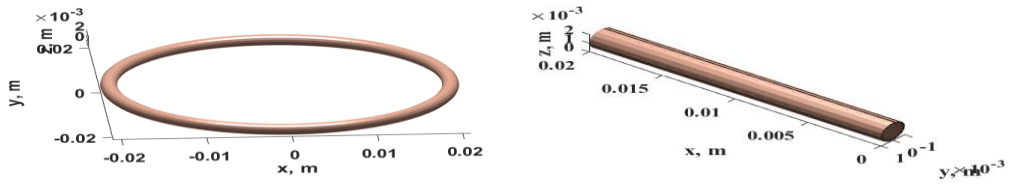

a) b)

Figure 16: Single conductor coil model

Figure 16 depicts the single conductor coil model, which includes (a) a single ring coil sample with 1A of total current and (b) a straight conductor with 1 A of total current. After building and designing the single ring coil conductor model, we write matlab scripts that can display and generate both a CAD surface mesh and a computational wire grid for a figure eight single planar coil with a total current of 1 A, as shown in the figure 17 below.

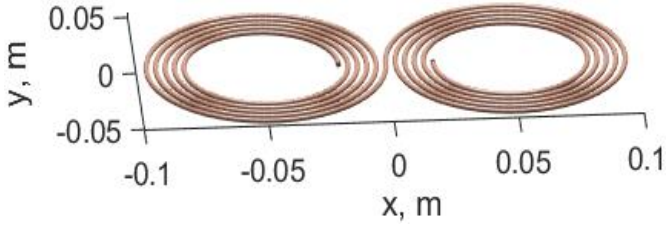

Figure 17: Figure eight type single planar Coil CAD design

Using the matlab script, we also generate the mesh (CAD surface mesh and computational wire grid) for a figure eight double planar coil with an entire current of 1 A. Figure 18 depicts the matlab script simulation results for the figure-eight shape double planar coil model with 1A conductor current.

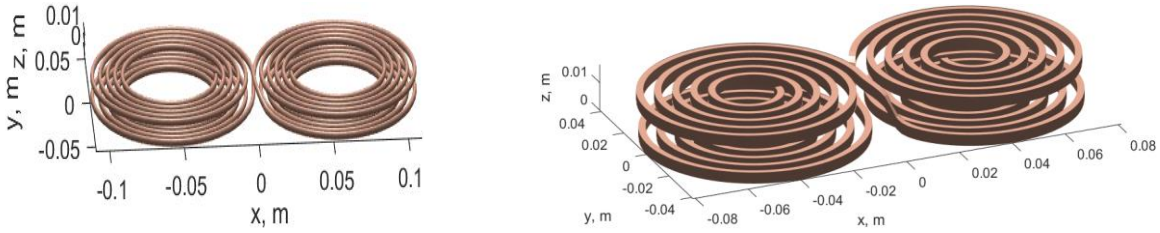

Figure 18: Figure eight double planar coil with 1 A of total current

A TMS magnetic coil model with relative current strength describes the intensity of the coil's magnetic pulses. The relative current strength controls the amplitude of generated electrical currents in brain tissue, which can alter TMS's effects on neuronal activity. Different TMS coil models have varying current strengths, which can be modified to meet research or therapeutic needs. Higher current strengths, for example, can be utilized to target deeper brain regions or elicit stronger neural responses, whilst lower current strengths may suffice for more superficial stimulation or specific experimental techniques. Researchers and doctors can change pulse amplitude, frequency, and length to control the TMS coil's relative current strength.

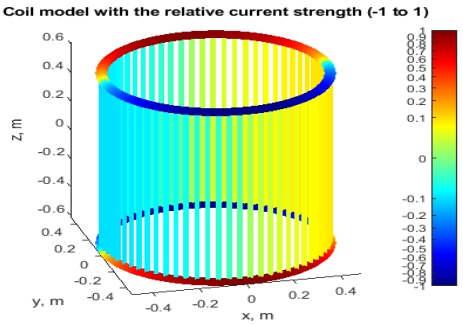

Figure 19: Coil model with relative current strength distribution

Figure 19 shows that the single ring conductor with the 1A current strength distributions. A coil model with relative current strength distribution is a depiction of a coil that takes into consideration the variation in current strength along its length. This information is critical for understanding the coil's magnetic field and how it interacts with other things.

4.4 Coil Positioning for different Brain Compartment

The optimum coil location for TMS varies according to the target brain compartment. For instance, to stimulate the dorsolateral prefrontal cortex, place the coil above the F3 position of the 10-20 lead EEG system [47], [48]. Due to specific differences in brain anatomy, it is critical to find the best coil position for each participant.

In coil position, we understand the qualities of brain tissue, the coil time-varying currents dI/dt of the tissues, and the steady-state currents. The coil position above the head model is defined by calculating the magnetic field and utilizing the correct rotation and translation. Coil rotation about its axis, tilt, and translation are related actions that are conducted to present the integrated brain model compartments - coil geometry, which includes the skull, skin, GM, WM, and CSF, as seen in the figure 20 below. The coil time-varying current dI/dt of the brain tissue defined for electric field is **9.4e7 Amperes/sec,** which may be written as the equation: **dI/dt= 2*pi*I0/period**. The time period is the inverse of the frequency of the distributed current, which is usually employed in TMS design, and the starting sample current/steady-state current, which is required to calculate the magnetic field, is **I0=5e3 Amperes**.

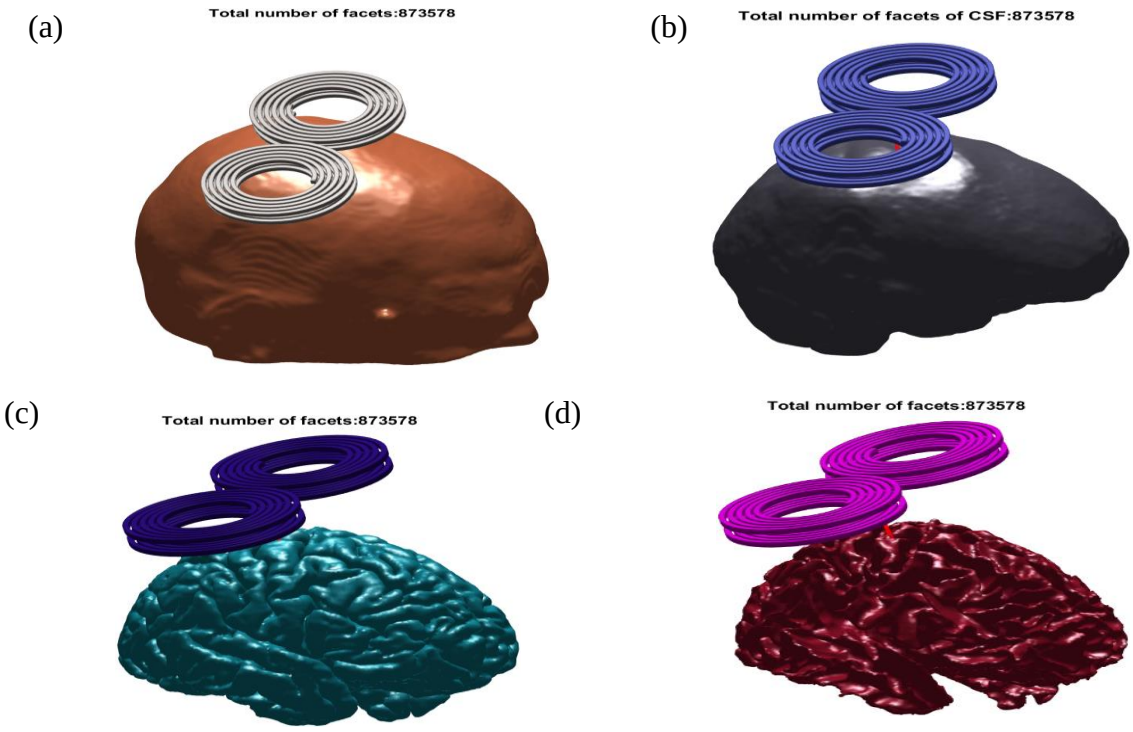

Figure 20: Brain compartments coil location (assigns coil position)

The figure 20 shows simulation outputs of distinct brain sections (a) Skull coil -geometry, (b) CSF coil geometry, (c) GM coil geometry, and (d) WM coil geometry

4.5 The induced magnetic field magnitude distributed on the brain compartments

Compute the B-field for brain tissue layers using the input values mentioned above (dI/dt, I0, and frequency). The matlab simulation outputs show that the magnetic field in the brain compartments varies between 0.1T to 0.8T for the skin, less than 0.06T to 0.5T for the skull, less than 0.05T to 0.4T for the CSF, less than 0.06T to 0.25T for WM and less than 0.05T to 0.3T for the GM, respectively.

In general, as we can see from the mat lab simulation outputs of various brain tissues, the magnitude of the magnetic field decreases as tissue depth increases, indicating that the field from the exterior tissue layer (skin) is greater than that from the inside tissue layers (gray matter).

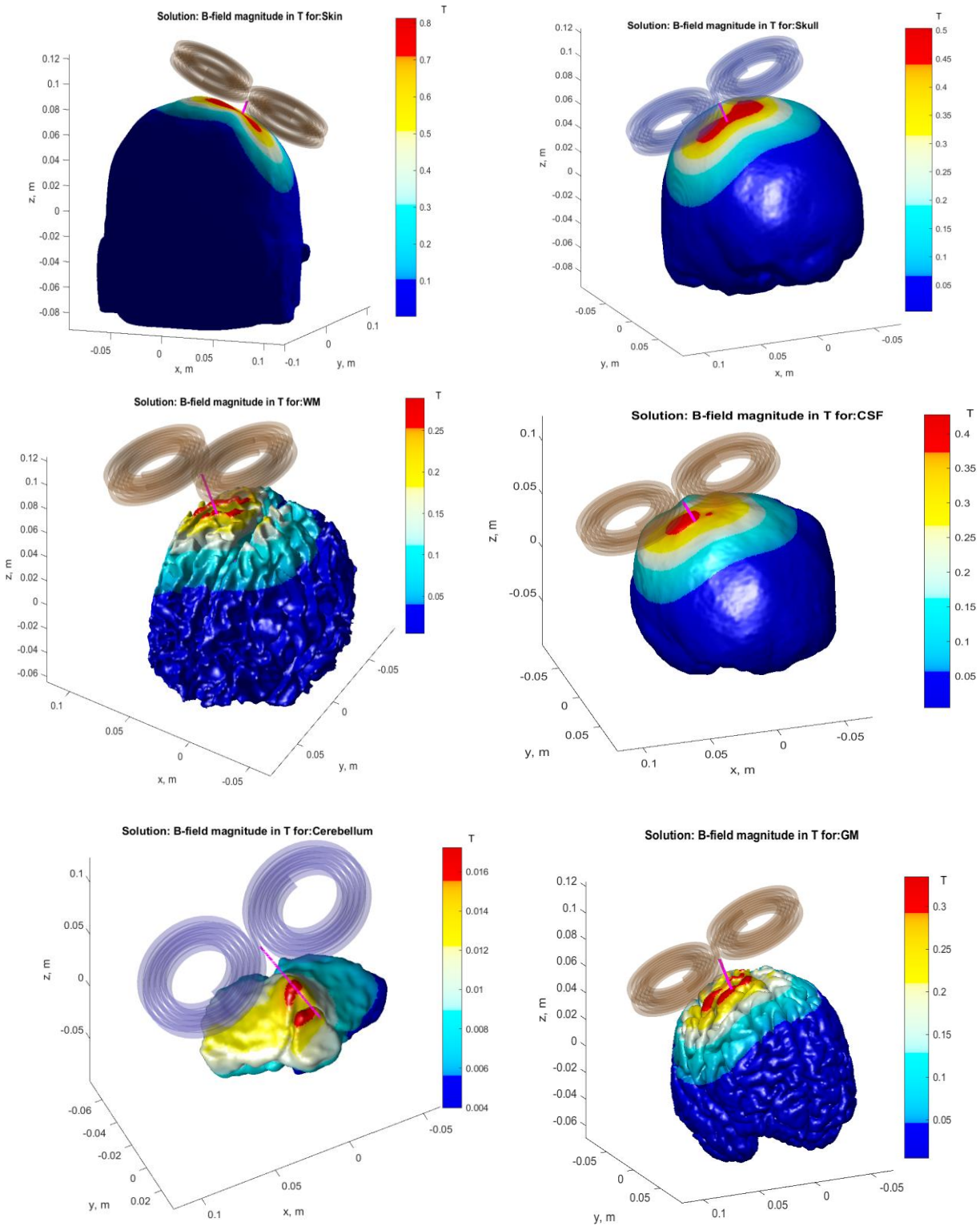

Figure 21: Magnitude of magnetic field distribution in brain compartments

In the figure 21 represents the magnetic field distribution and its magnitude of all brain compartments (skin, skull, WM, CSF, cerebellum, and GM).

4.6 Induced surface charge density in Brain compartments

Induced surface charge density is defined as the accumulation of electric charge on a material's surface caused by an external electric field. It results from the movement of free electrons within the material in reaction to the field.

In this section, we use BEM/FMM iterative solutions to calculate the induced surface charge density for brain tissue layers in an external time-varying magnetic field generated by a coil. Based on this, the solution can have up to four iterations. To estimate the induced surface charge density of brain tissue layers, we employ a mathematical model based on charge conservation laws (argues that the total electric charge in a closed system is constant, that means charge cannot be created or destroyed; it can only be transferred between objects).

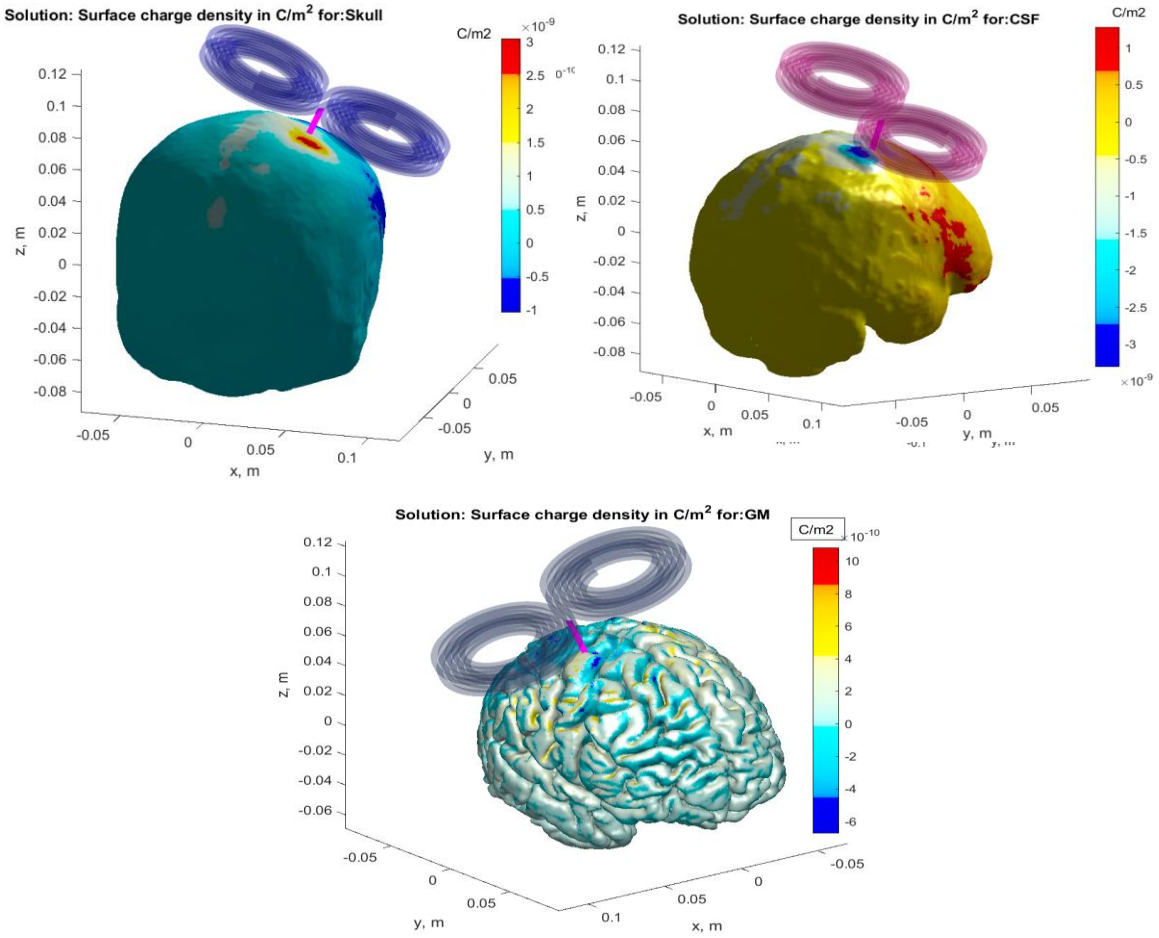

Figure 22: Induced surface charge density simulation outputs of Brain compartments

4.7 Electric field within and outside of Brain compartments surface

The electric field within the brain is a complex and dynamic phenomenon that is essential for a variety of neurological activities such as neuronal communication, information processing, and cognitive function. The electric field's strength and distribution vary according to brain activity, stimulation modalities, and individual brain structure.

The electric field outside the brain can be influenced by a variety of factors, including transcranial magnetic stimulation (TMS). These external electric fields can penetrate the skull and modulate neuronal activity, potentially altering cognitive functions and behavior. We simulate and compute the magnitude of the brain compartment's electric field strength using the MATLAB configuration software tools based on the BEM-FMM functionalities. This is where the overall electric fields of the various brain shells are calculated, just inside and outside.

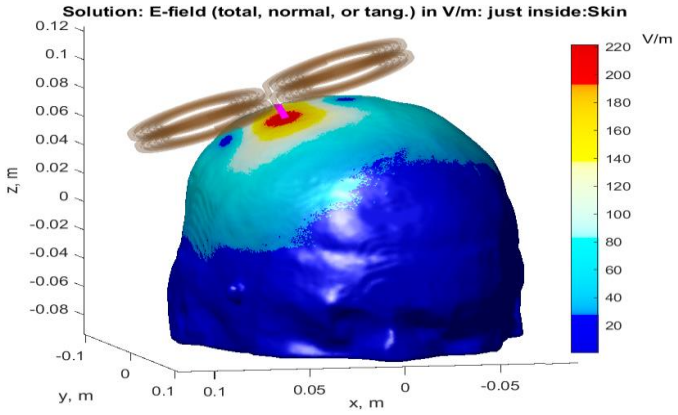

MAX E total: 221.8663V/m

MAX E normal: 15.2713 V/m

MAX E tangent: 221.6439 V/m

Figure 23: Magnitude of the total electric field just within the skin shell

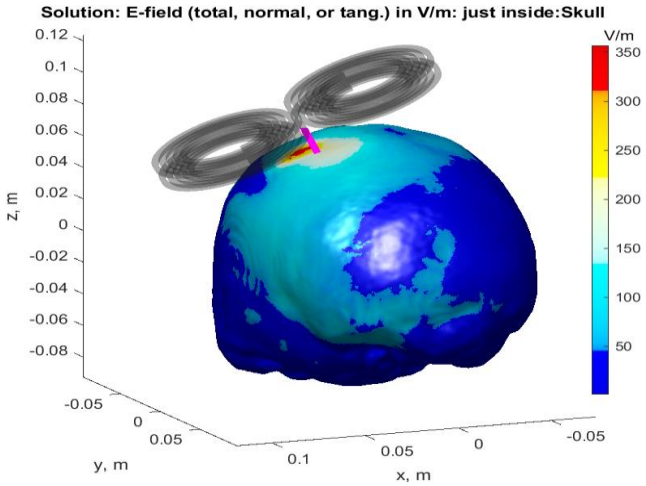

MAX E total: 356.6508V/m

MAX E normal: 345.7989 V/m

MAX E tangent: 150.9812 V/m

Figure 24: Magnitude of the total electric fields just within the skull shell

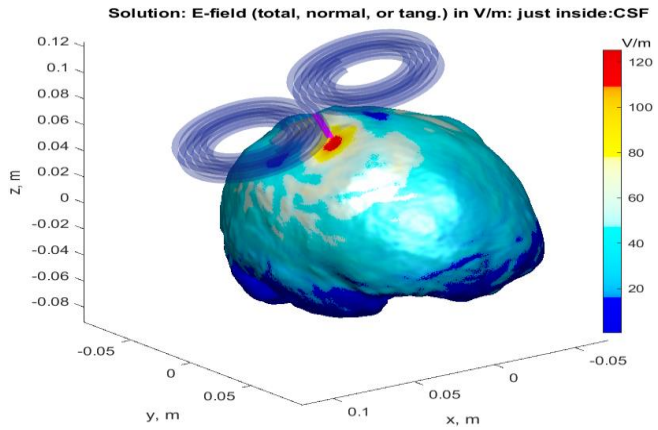

MAX E total: 125.3758 V/m

MAX E normal: 16.7182 V/m

MAX E tangent: 125.3753 V/m

Figure 25: Magnitude of the total electric fields just inside the CSF shell

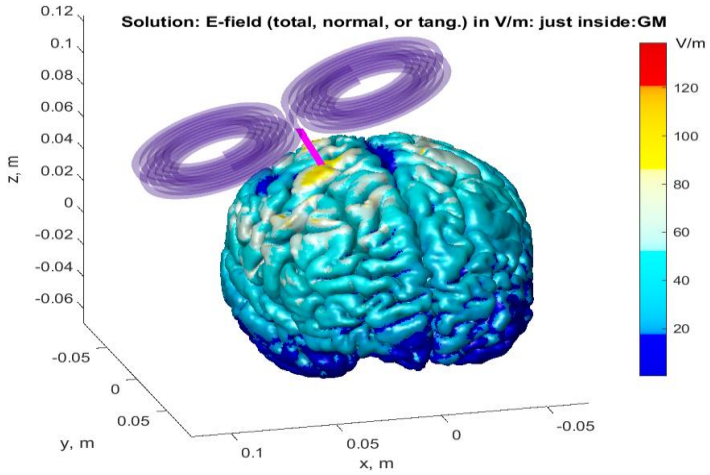

MAX E total: 138.6670

MAX E normal: 138.4590

MAX E tangent: 112.9445

Figure 26: Magnitude of the total electric fields just inside the GM shell

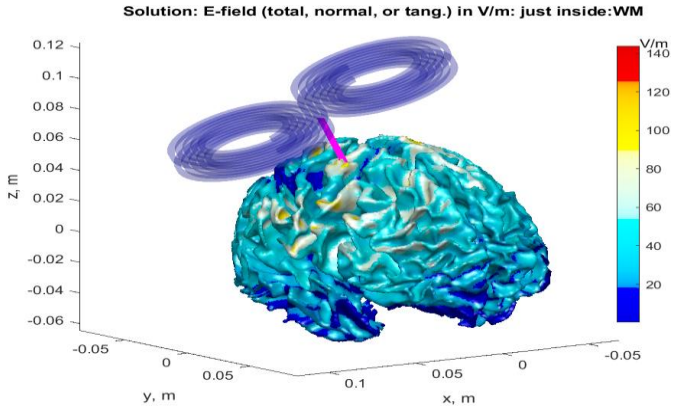

MAX E total: 143.8066

MAX E normal: 143.7395

MAX E tangent: 96.7054

Figure 27: Magnitude of the total electric fields just inside the WM

4.8 Computes and plot the Lorentz force

The Lorentz force is defined as an interaction of magnetic and electric forces acting on a point charge via electromagnetic fields. It is used in electromagnetism, sometimes called

electromagnetics, to apply force to a charged particle passing through a magnetic field. It is defined by the equation: **F = q (v x B),** where F is the force, q is the particle's charge, v is its velocity, and B is the magnetic field. Particle accelerators use the Lorentz force to speed up charged particles at high rates of speed. A particle accelerator uses an electric field to accelerate particles and a magnetic field to guide their trajectory. Scientists and researchers examine fundamental particles and forces by carefully adjusting the strength and direction of both the electric and magnetic fields. The Lorentz force is critical in ensuring that particles go in the appropriate direction within the accelerator.

From this portion we calculate and depict the Lorentz force (N/m^2) on a charged particle inside or outside a brain compartment surface, including the surface field and coil geometry.

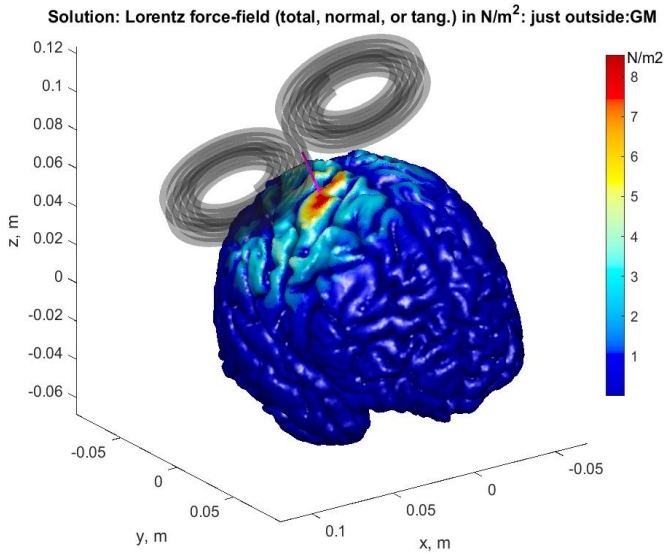

MAX F total: 8.5 N/m2

MAX F normal: 8.5 N/m2

MAX F tangent: 6.4 N/m2

Figure 28: Distribution and magnitude of Lorentz force on GM

4.9 Compute the Electric potential of Brain compartments

Electric potential is the amount of work energy required to transmit one unit of electric charge from a reference point to a given location in an electric field. Electric potential energy is the energy that a charged object has because of its position in an electric field. It is the amount of energy required to move an object from its current position to a reference point with zero potential. Electric potential is the amount of energy available per unit charge at a given place in a static electric field. This section calculates the electric potential

of the secondary field for any brain compartment surface (plots density and, optionally, coil geometry).

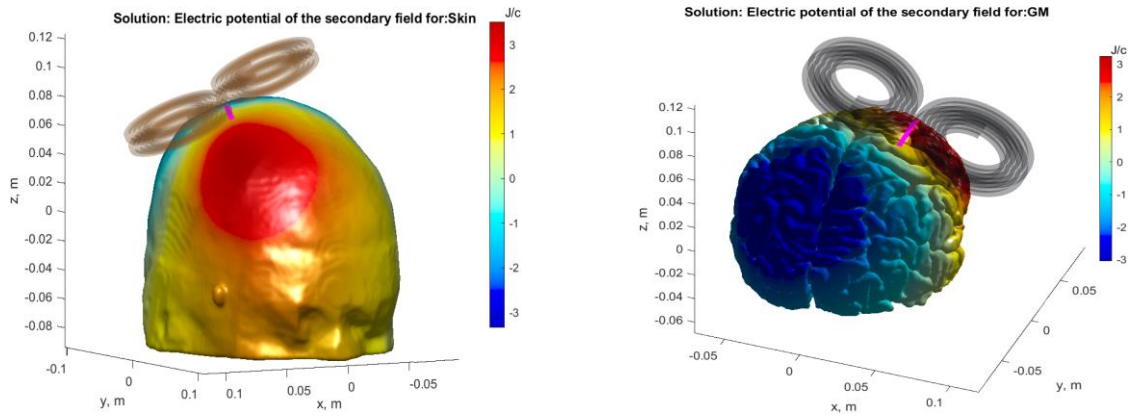

Figure 29: Electrical potential of the skin and GM brain compartments

4.10 Cross-sectional and planes of Brain

Generally, the brain is divided into three primary planes: axial (which divides top and bottom), coronal (which divides front and back), and sagittal (which divides left and right). These sections provide many viewpoints on the structure of the brain, each disclosing particular details about its composition and arrangement.

4.10.1 Different cross-sections and planes of the Brain layers of the NIfTI data

While the brain has a structure that is three-dimensional, every position within it can be localized on one of three planes: x, y, or z. The precise position can be determined using three planes: coronal (vertical, dividing front and back), horizontal (top and bottom), and sagittal (left and right).

Here we create a matlab script that defines three observation planes and plots cross-sections and NIfTI data when available. In this procedure, we use cross-sectional information to enable quick (real-time) presentation and develop a matlab script to discover all edges and attached triangles for individual brain compartments. The script is required for the following visualizations:

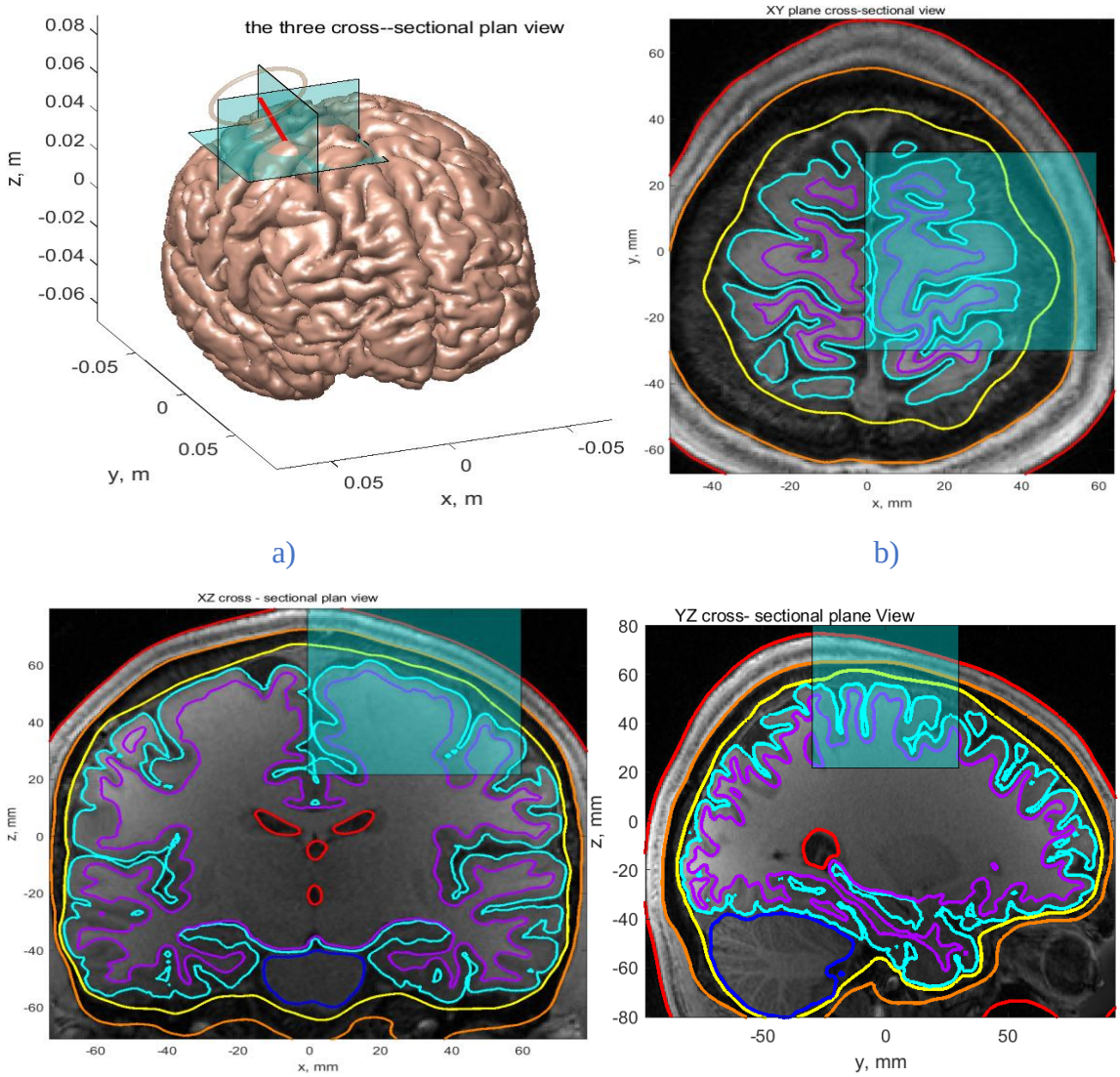

Figure 30: Cross- sectional view of the brain in different plane

Figure 30 illustrates the cross- sectional view of brain in different plans (a) the three (X, Y & Z) sectional plane view of the brain, (b) XY cross sectional plane view, (c) XZ cross sectional plane view and (d) YZ cross sectional view of the brain.

4.11 Computing magnetic and electric fields distribution of the coil on different plane surface

The distribution of a magnetic field over a surface varies depending on the source of the field and the surface's qualities. In general, the shape and size of the object generating the

field, the existence of additional magnetic materials, and the distance from the source can all have an impact on the distribution of the magnetic field throughout the surface.

The magnetic field distribution over a surface (transverse plane) in the x-component due to a TMS coil can be estimated using the basic FMM approach. This method involves discretizing the coil geometry into small elements and then calculating Maxwell's equations to determine the magnetic field at each element.

For this work, we use the following basic parameters in matlab simulations: the TMS coil is driven with a time-varying current of $dI/dt = 9.4e7\ Amperes/sec$, conductor current of 5 kA and a CW frequency of 3 kHz.

Here bellow in figure 31 shows that the distribution magnetic field distribution of the TMS coil over transvers plane in x-component. The magnitude of the field strength shows that in different colors levels, the yellow color field show that the high intensity level which measures up to 36 T.

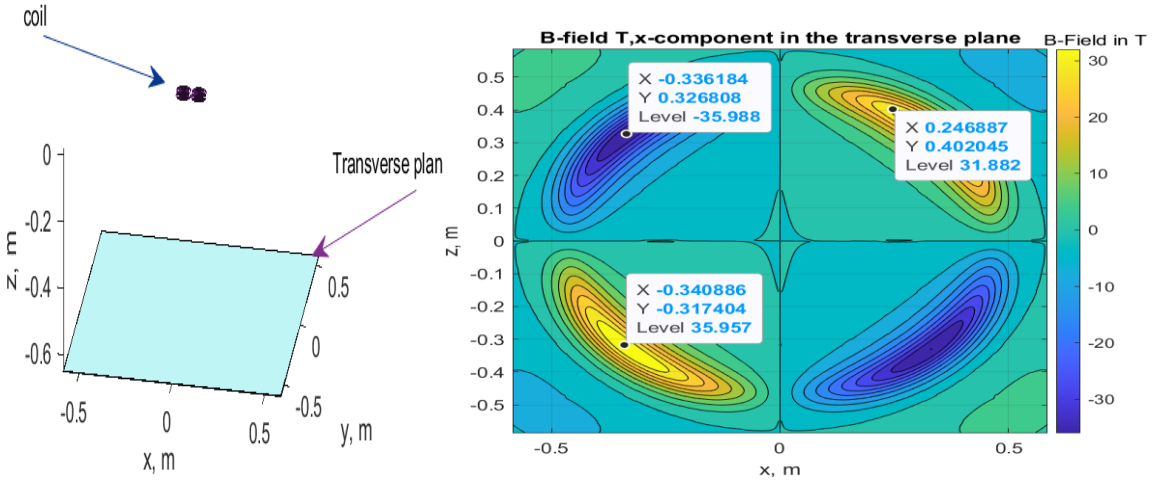

Figure 31: Distribution of B-field in the X-component of transvers plane

The electric field distribution of the TMS coil on distinct human brain surfaces is critical in many cognitive tasks, including memory, attention, and decision-making. It is produced by the activity of neurons, which communicate with one another by electrical and chemical impulses. The figures bellow shows the E-field distribution of the brain layers in different plans.

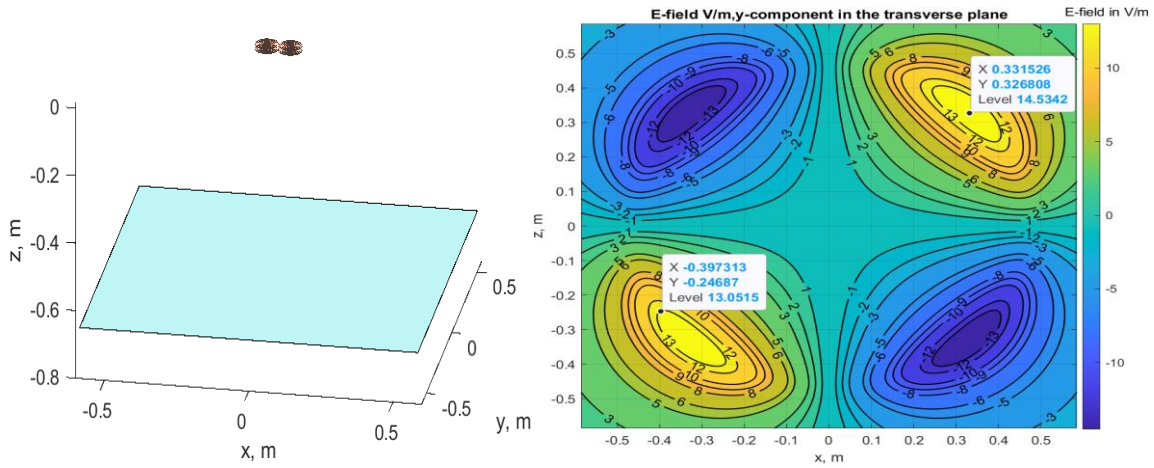

(a) (b)

Figure 32: Distribution of E-field in the y-component of transvers plan

The figure 32 above shows that distribution of electric field in the transvers plan (a) shows the y- transvers plane position of the coil and (b) the distribution of E-field in y- transvers plane.

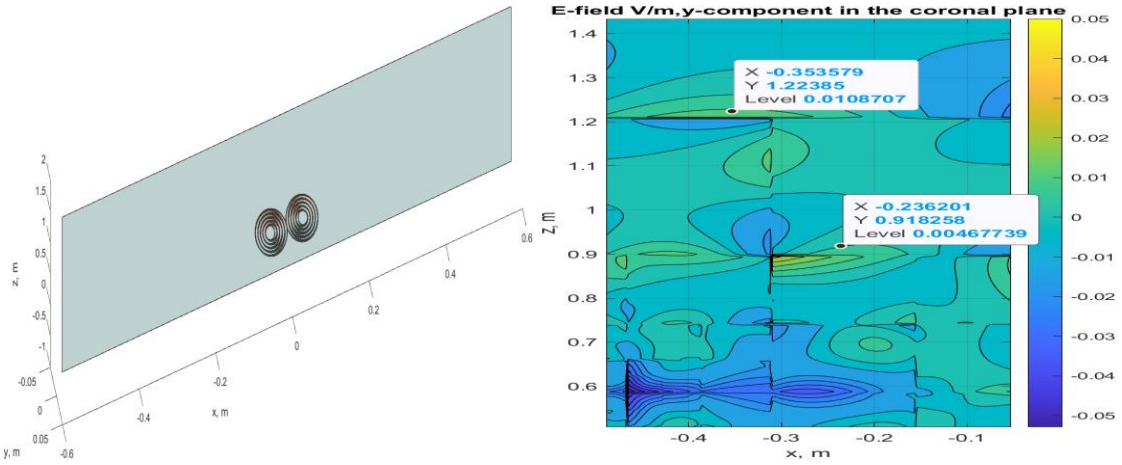

(a) (b)

Figure 33: Distribution of E-field in the y-component of coronal plan

Figure 33 represents the distribution of electric field in the coronal plan, (a) shows the y-coronal plane position of the coil and (b) the distribution of E-field in y- coronal plane.

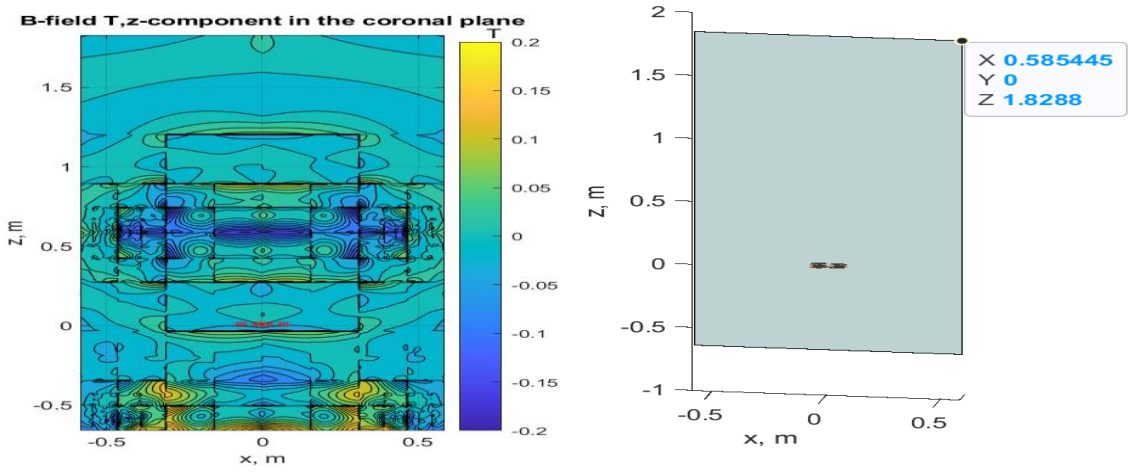

Figure 34: Distribution of B-field in the Z-component of coronal plane

The figure 34 represents the distribution of magnetic field the coronal plane z-component and accurately computes and displays magnetic field sampled over a surface (coronal plane) due to a coil via the plain FMM method.

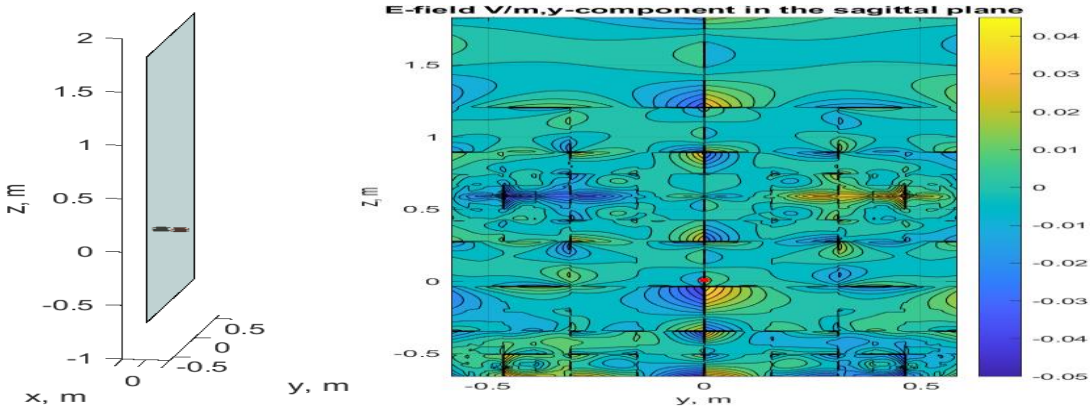

Figure 35: Distribution of E-field in the y-component of sagittal plane.

Figure 35 above represents the spatial distribution of the electric field in the sagittal plane's y-component and computes and illustrates the electric field sampled over a surface (sagittal plane) due to a coil using the basic FMM approach.

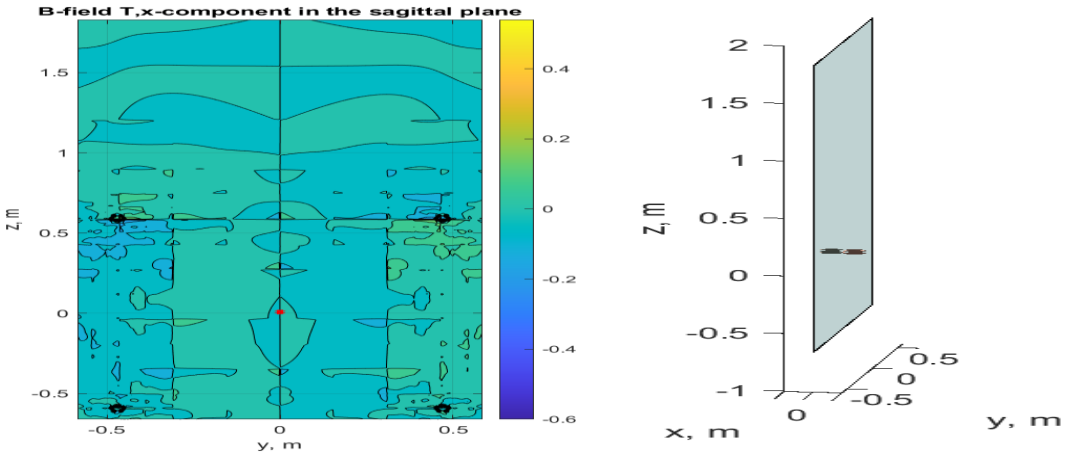

Figure 36: Distribution of E-field in the y-component of sagittal plane

Figure 36 emphasizes the spatial distribution of E-field in the y-component of the sagittal plan, that computes and displays the electric field sampled over a surface (sagittal plane) due to a coil using the basic FMM approach.

4.12 Coil tester line magnetic and electric field

A coil tester analyzes coil performance and integrity. Figure 35 illustrates the MATLAB outputs of the TMS figure eight type coil magnetic field in the x, y, and z planes, which are red Bx, magenta By, and blue Bz. The Outputs are the total magnetic field (or any of the field components) along the line given I0 A of conductor current with the basic parameters which include magnetic permeability of vacuum(~air), and coil parameters (I0=5e3A for magnetic field). Also, figure 38 illustrates the mat lab outputs of the TMS figure eight type coil electric field in the x, y, and z planes, which are red Ex, magenta Ey, and blue Ez. The Outputs are solenoidal electric field dA/dt (or any of the field components) along the line given I0 A of conductor current and frequency.

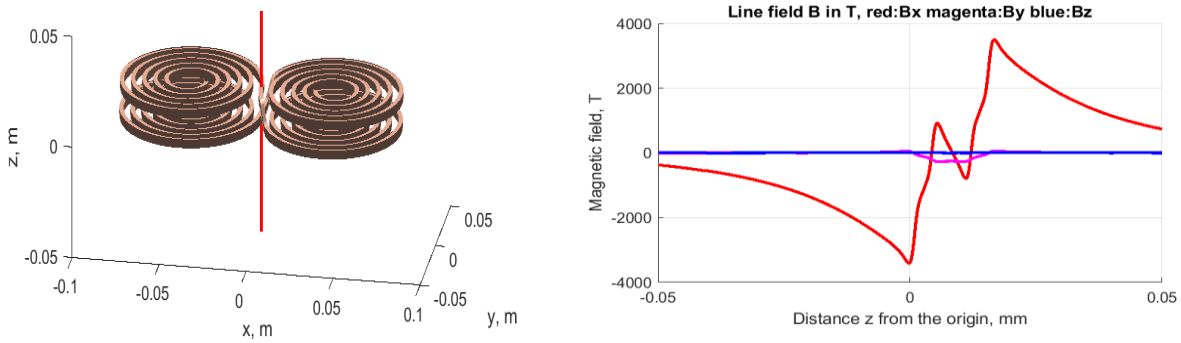

Figure 37: TMS coil tester line for magnetic field

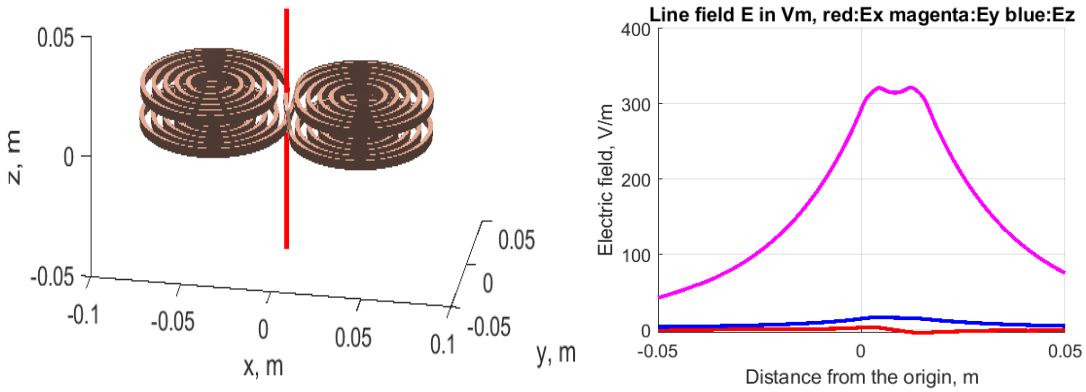

Figure 38: TMS coil tester line for Electric field

Figures 37 and 38 depict the coil tester line's magnetic and electric fields, respectively, with the left side representing the coil tester line and the right-side representing field outputs.

Chapter Five

Conclusion, Recommendation and Future Work

The primary goal of this thesis is to design, simulate and analysis of the TMS system which is used for MDD recovery. The TMS system design is focusing on the basic components which includes the coil design and compute the computational distribution effects of the electromagnetic fields and other components, these includes charge density, Lorentz force, magnetic and electric fields using the BEM-FMM computational model that increase the accuracy, precision, optimizing the coil placement on the human brain compartments and also reduce the computation time. In addition to the basic tasks that we mentioned in the above paragraph in this thesis we also investigate and analyze the prevalence rate and current treatment challenges of major depression disorder in the local community by collecting numerical data from two highly populous psychiatric disorder-examining hospitals, Felege Hiwot Specialized and Tibebe Ghion Teaching Hospitals. So, based on the one-year data collected in the two hospitals, the prevalence rate of MDD is higher in females as compared to males, as evidenced by the 978 total cases of newly arrived MDD patients (523, which is 53.5% females, and 455, which is 46.5% males).

After investigating the prevalence rate, we revied different brain stimulation experiments, neuroimaging and neuropsychiatric evidence to understand the basic parts of human brain mostly affected by MDD. According to conclusion from neuroimaging, neuropsychiatric, and brain stimulation research, MDD primarily affects the following brain structures: frontal lobe, amygdala, hippocampus, thalamus, and parental lobes.

To design, simulate and analyze computational models of the head, we first created and examined all of the basic brain compartments and developed the mathematical model. The data for each brain compartment is being generated using simNIBS and matlab software pipelines. After identifying each brain compartment, we simulate and analyze the TMS coil position by assigning basic parameters such as the sample field margin(the boundary line or the area immediately inside the boundary) is 0.8, the coil time-varying current dI/dt of the brain tissue, which is defined for an electric field of 9.4e7 amperes/sec, and the sample current/steady-state current, which is required to calculate the magnetic field, I0 = 5e3 Amperes, permittivity, conductivity of each brain layer and the best position of coil

placement of each compartment. We compute, simulate, and analyze the induced magnetic field, total electric field, induced surface charge density, and Lorentz force of each brain layer using the fundamental parameters and BEM-FMM toolkits that are integrated in matlab.

Based on our BEM-FMM computational model simulation outputs, we conclude that the magnitude of the induced magnetic field of the brain compartment decreases as tissue depth increases, indicating that the field from the exterior tissue layer (skin) is greater than that from the inside tissue layers (gray matter). Matlab simulation outputs show that the magnetic field in the brain compartments varies between 0.1T to 0.8T for the skin, less than 0.06T to 0.5T for the skull, less than 0.05T to 0.4T for the CSF, and less than 0.05T to 0.3T for the GM, respectively. TMS coil magnetic and electric field distribution in various brain compartments in different planes was simulated and analyzed. The coil's magnetic and electric fields change when the thickness of the brain compartment changes. The magnetic field magnitude ranges from 0 to 36T, as we seen our simulation outputs, whereas the electric field magnitude ranges from 0 to 15V/m.

In general, by the end of this thesis, psychiatric professionals should explore the benefits of employing a TMS system to treat MDD, which activates specific brain regions, perhaps improving activity and connectivity. This can help to improve cognitive skills like memory, attention, and language. In addition to the TMS computational model analysis, future research could focus on the design of electrical components using protocols, as well as the simulation and analysis of each brain neuron's electrical signal qualities before and after depression relief or therapy.

We recommend that health and engineering academic institutions educate hospital communities, health professionals, and psychiatric patients about the benefits of TMS for the treatment of MDD over antidepressant medicines.

Reference

[1] WHO publication, "draft Intersectoral Global Action Plan on Epilepsy and Other Neurological Disorders 2022–2031," 27 April 2022.

[2] B. Guilherme, A. William, N. Sergey and Axel Thielscher,, "Accurate TMS Head Modeling: Interfacing Simoni's and BEMFMM In A MATLAB-Based Module,," 22 september 2022.

[3] C. Lomen-Hoerth , Nervous System Disorders, G. Hammer , S. McPhee and Pathophysiology of disease:, "An Introduction to Clinical Medicine,," p. http:// access harmacy.mhmedical.com/content.aspx? bookid=961&sectionid=53555688, 30 November 2022.

[4] Timothy Wagner and Antoni Valero-Cabre Alvaro Pascual-Leone, "Noninvasive Human Brain Stimulation," Annual Review of Biomedical Engineering, pp. 527-56591 10.1146/annurev.bioeng.9.061206.13310017444810, 2007.

[5] W. H. Organization, "Depression and other common mental disorders: global health estimates.,"WorldHealthOrganization.https://apps.who.int/iris/handle/10665/254610, 2017.

[6] a. o. GBD 2015 Disease and Injury Incidence and Prevalence Collaborators, "Global, regional, and national incidence, prevalence, and years lived with disability for 310 diseases and injuries, 1990–2015," systematic analysis for the Global Burden of Disease Study , 2015.

[7] B. Dell'Osso, and G. Di Lorenzo, "Non-Invasive Brain Stimulation in Psychiatry and Clinical Neurosciences,," https://doi.org/10.1007/978-3-030-43356-7_1, AG 2020.

[8] Eldaief MC,, Press DZ, , Pascual and Leone A., "Transcranial magnetic stimulation in neurology," review of established and prospective applications, p. DOI: 10.1212/01.CPJ.0000436213.11132.8e. PMID: 4353923; PMCID: PMC3863979, 6 Dec 2013.

[9] Farzan, Faranak & Vernet, Marine & Shafi, Mouhsin & Rotenberg,, Alexander & Daskalakis and afiris & Pascual-Leone, Alvaro., "Characterizing and Modulating Brain Circuitry through Transcranial Magnetic Stimulation Combined with Electroencephalography. Frontiers in Neural Circuits.," 2016.

[10] WHO,,"DepressionRates by Country," https://worldpopulationreview.com/country-rankings/depression-rates-by-country, 2022.

[11] WHO,"depression,," https://www.who.int/news-room/fact-sheets/detail/depression, September 2021

[12] Bahman Zohuri, Patrick J. McDaniel., "Electrical brain stimulation for the treatment of neurological disorders," Canadiana (print) 0125098, 2019.

[13] G. Bicalho Saturnino, "Computational Modelling and Optimization of Electric Fields Generated by Transcranial Brain Stimulation," DTU Health Technology, 2020.

[14] M. D. A. V. P. Luis J. Gomez, "Fast computational optimization of TMS coil placement for individualized electric field targeting,"DOI: https://doi.org/10.1101/2020.05.27.120022, 2020.

[15] E. G. L. R. L. H. a. D. C. J. P. Rastogi, "Transcranial Magnetic Stimulation-coil design with improved focality;," https://doi.org/10.1063/1.4973604, 2017

[16] W. M. G. A. V. P. Aman S. Aberra Boshuo Wang b, "Simulation of transcranial magnetic stimulation in head model with morphologically-realistic cortical neurons;," Https://Www.Sciencedirect.Com/Journal/Brain- Stimulation?, April 2021.

[17] G. M. N. E. H. B. D. N. P. A. T. H. L. N. d. L. T. R. A. N. Sergey N. Makarov, "Software Toolkit for Fast High-Resolution TMS Modeling," DOI: https://doi.org/10.1101/643346, May 2019

[18] G. Bicalho Saturnino, "Computational Modelling and Optimization of Electric Fields Generated by Transcranial Brain Stimulation.," DTU Health Technology, 2020.

[19] M. Guidetti, A. Bertini, F. Pirone, G. Sala, P. Signorelli, C. Ferrarese, A. Priori and T. Bocci, "Neuroprotection and Non-Invasive Brain Stimulation:," https://doi.org/10.3390/ijms232213775, 23 july 2022

[20] W. T. M. P. N. M. P. W. L. S. P.-L. A. B. M. Peterchev AV, "Fundamentals of transcranial electric and magnetic stimulation dose," definition, selection, and reporting practices., p. DOI: 10.1016/j.brs.2011.10.001. Epub 2011 Nov 1. PMID: 22305345; PMCID: PMC3346863., 1 Nov 2012.

[21] D. Q. Truong, ""Translational Modeling of Non-Invasive Electrical Stimulation"," CUNY Academic Works: https://academicworks.cuny.edu/cc_etds_theses/774, 2019

[22] W. W. M. S. T. A. Saturnino GB, "Accurate TMS Head Modeling: Interfacing SimNIBS and BEM-FMM in a MATLAB-Based Module.," Annu Int Conf IEEE Eng Med Biol Soc.doi: 10.1109/EMBC44109.2020.9175802. PMID: 33019186., pp. 326-5329, Jul 2020.

[23] https://www.cambridge.org//academic/subjects/engineering/engineering, "mathematics and programming/fast-multipole-boundary-element-method-theory-and-applications-engineering?," format=HB&isbn=9780521116596, 2022.

[24] B. A. C. Bikson M and Clark VP, Cohen LG,, "Rigor and reproducibility in research with transcranial electrical stimulation:," An NIMH-sponsored workshop. Brain Stimul, pp. 465-480, 13 Dec 2018.

[25] Saturnino GB,, Wartman WA, and Makarov SN, "Accurate TMS Head Modeling: Interfacing SimNIBS and BEM-FMM in a MATLAB-Based Module.," Annu Int Conf IEEE Eng Med Biol Soc. doi: 10.1109/EMBC44109.2020.9175802, pp. 5326-5329, Jul 2020.

[26] S. N. Makarov, W. A. Wartman, M. Daneshzand, K. Fujimoto, T. Raij, and A. Nummenmaa, “A software toolkit for TMS electric-field modeling with boundary element fast multipole method: an efficient MATLAB implementation,” J. Neural Eng., vol. 17, no. 4, p. 046023, Aug. 2020, doi: 10.1088/1741-2552/ab85b3.

[27] L. J. Gomez, M. Dannhauer, and A. V. Peterchev, “Fast computational optimization of TMS coil placement for individualized electric field targeting,” NeuroImage, vol. 228, p. 117696, Mar. 2021, doi: 10.1016/j.neuroimage.2020.117696.

[28] F. Zhang, W. Peng, J. A. Sweeney, Z. Jia, and Q. Gong, “Brain structure alterations in depression: Psych radiological evidence,” CNS Neurosis. Ther., vol. 24, no. 11, pp. 994–1003, Mar. 2018, doi: 10.1111/cns.12835.

[29] “What causes depression?” Harvard Health. Accessed: May 07, 2023. https://www.health.harvard.edu/mind-and-mood/what-causes-depression

[30] M. Pandya, M. Altinay, D. A. Malone, and A. Anand, “Where in the Brain Is Depression?” Curr. Psychiatry Rep., vol. 14, no. 6, pp. 634–642, Dec. 2012, doi: 10.1007/s11920-012-0322-7.

[31] J. Repple et al., “Severity of current depression and remission status are associated with structural connectome alterations in major depressive disorder,” Mol. Psychiatry, vol. 25, no. 7, Art. no. 7, Jul. 2020, doi: 10.1038/s41380-019-0603-1.

[32] “Thalamus - an overview | ScienceDirect Topics.” Accessed: May 08, 2023. [Online]. Available: https://www.sciencedirect.com/topics/neuroscience/thalamus

[33] M. E. Mel’nikov et al., “fMRI Response of Parietal Brain Areas to Sad Facial Stimuli in Mild Depression,” Bull. Exp. Biol. Med., vol. 165, no. 6, pp. 741–745, Oct. 2018, doi: 10.1007/s10517-018-4255-y.

[34] E. Okada and D. T. Delpy, “Near-infrared light propagation in an adult head model II Effect of superficial tissue thickness on the sensitivity of the near-infrared spectroscopy signal,” Appl. Opt., vol. 42, no. 16, p. 2915, Jun. 2003, doi: 10.1364/AO.42.002915.

[35] K. A. Sathi, Md. K. Hosain, and Md. A. Hossain, “Analysis of Induced Field in the Brain Tissue by Transcranial Magnetic Stimulation Using Halo-V Assembly Coil,” Neurol. Res. Int., vol. 2022, pp. 1–10, Jul. 2022, doi: 10.1155/2022/7424564.

[36] S. Bai, S. Dokos, K.-A. Ho, and C. Loo, “A computational modelling study of transcranial direct current stimulation montages used in depression,” NeuroImage, vol. 87, pp. 332–344, Feb. 2014, doi: 10.1016/j.neuroimage.2013.11.015

[37] S. Bai, S. Dokos, K.-A. Ho, and C. Loo, “A computational modelling study of transcranial direct current stimulation montages used in depression,” NeuroImage, vol. 87, pp. 332–344, Feb. 2014, doi: 10.1016/j.neuroimage.2013.11.015.

[38] Jose Gomez-Tames et al, “Review on biophysical modelling and simulation studies for transcranial magnetic stimulation” 2020 Phys. Med. Biol. 65 24TR03

[39] Clemente Cobos Sánchez et al,” Design of TMS coils with reduced Lorentz forces: application to concurrent TMS-fMRI” 2020 J. Neural Eng. 17 016056

[40] Konakanchi, D.; de Jongh Curry, A.L.; Waters, R.S.; Narayana, S. Focality of the Induced E-Field Is a Contributing Factor in the Choice of TMS Parameters: Evidence from a 3D Computational Model of the Human Brain. Brain Sci. **2020**, 10, 1010. https://doi.org/10.3390/brainsci10121010

[41] Konstantin Weise, Ole Numssen, Axel Thielscher, Gesa Hartwigsen, Thomas R. Knösche,A novel approach to localize cortical TMS effects, NeuroImage, Volume 209,2020,116486,ISSN1053, https://doi.org/10.1016/j.neuroimage.2019.116486

[42] Maria Drakaki, Claus Mathiesen, Hartwig R. Siebner, Kristoffer Madsen, Axel Thielscher, Database of 25 validated coil models for electric field simulations for TMS, Brain Stimulation, Volume 15, Issue 3, 2022, Pages 697-706,ISSN 1935-861X, https://doi.org/10.1016/j.brs.2022.04.017

[43] Alexander et.al, Physiological observations validate finite element models for estimating subject-specific electric field distributions induced by transcranial magnetic stimulation of the human motor cortex, NeuroImage, Volume 81, 2013, Pages 253-264, ISSN 1053-8119, https://doi.org/10.1016/j.neuroimage.2013.04.067.

[44] K. A. Sathi, M. A. Hossain, M. K. Hosain, N. H. Hai and M. A. Hossain, "A Deep Neural Network Model for Predicting Electric Fields Induced by Transcranial Magnetic Stimulation Coil," in IEEE Access, vol. 9, pp. 128381-128392, 2021, doi: 10.1109/ACCESS.2021.3112612.

[45] Gomez-Tames, J., Laakso, I., Murakami, T., Ugawa, Y., & Hirata, A. (2020). TMS activation site estimation using multiscale realistic head models. Journal of Neural Engineering. doi:10.1088/1741-2552/ab8ccf

[46] Afuwape, Oluwaponmile F., Olumide O. Olafasakin, and David C. Jiles. "Neural network model for estimation of the induced electric field during transcranial magnetic stimulation." IEEE Transactions on Magnetics 58, no. 2 (2021): 1-5.

[47] Bader, Oliver et al. “cyp51A-Based mechanisms of Aspergillus fumigatus azole drug resistance present in clinical samples from Germany.” Antimicrobial agents and chemotherapy vol. 57,8 (2013): 3513-7. doi:10.1128/AAC.00167-13

[48] Janssen, A.M., Oostendorp, T.F. & Stegeman, D.F. The coil orientation dependency of the electric field induced by TMS for M1 and other brain areas. J NeuroEngineering Rehabil **12**, 47 (2015). https://doi.org/10.1186/s12984-015-0036-2

[49] Koponen, L.M., Stenroos, M., Nieminen, J.O. et al. Individual head models for estimating the TMS-induced electric field in rat brain. Sci Rep **10**, 17397 (2020). https://doi.org/10.1038/s41598-020-74431-z

[50] Deng Z-D, Robins PL, Dannhauer M, Haugen LM, Port JD, Croarkin PE. Optimizing TMS Coil Placement Approaches for Targeting the Dorsolateral Prefrontal Cortex in Depressed Adolescents: An Electric Field Modeling Study. Biomedicines. 2023; 11(8):2320. https://doi.org/10.3390/biomedicines11082320

[51] Owzareck, Michael, Lüning, Kai, and Parspour, Nejila. ‘Optimization of a Single Strip Tester to Measure Magnetic Properties of Electrical Sheet Steel at Medium Frequencies’. 1 Jan. 2019: S67 – S72

[52] Mandziuk, M., Ball, L., and Piper, S., "Application of Transient Magnetic Fields to a Magnetosensitive Device," SAE Int. J. Passeng. Cars – Electron. Electr. Syst. 11(3):183-195, 2018, https://doi.org/10.4271/2018-01-1349

[53] S. Ploumpis *et al.*, "Towards a Complete 3D Morphable Model of the Human Head," in *IEEE Transactions on Pattern Analysis and Machine Intelligence*, vol. 43, no. 11, pp. 4142-4160, 1 Nov. 2021, doi: 10.1109/TPAMI.2020.2991150

[54] Yoon SY, Hunter JE, Chawla S, Clarke DL, Molony C, O'Donnell PA, Bagel JH, Kumar M, Poptani H, Vite CH, Wolfe JH. Global CNS correction in a large brain model of human alpha-mannosidosis by intravascular gene therapy. Brain. 2020 Jul 1;143(7):2058-2072. doi: 10.1093/brain/awaa161. PMID: 32671406; PMCID: PMC7363495.